

# Lifetime measurements and oscillator strengths in singly ionised scandium and the solar abundance of scandium

A. Pehlivan Rhodin<sup>1,2</sup><sup>★</sup>, M. T. Belmonte<sup>3</sup>, L. Engström<sup>4</sup>, H. Lundberg<sup>4</sup>, H. Nilsson<sup>1</sup>, H. Hartman<sup>1,2</sup>, J. C. Pickering<sup>3</sup>, C. Clear<sup>3</sup>, P. Quinet<sup>5,6</sup>, V. Fivet<sup>5</sup>, and P. Palmeri<sup>5</sup><sup>†</sup>

<sup>1</sup>*Lund Observatory, Lund University, PO Box 43, SE-221 00 Lund, Sweden*

<sup>2</sup>*Materials Science and Applied Mathematics, Malmö University, 205 06 Malmö, Sweden*

<sup>3</sup>*Physics Department, Blackett Laboratory, Imperial College London, London SW7 2BZ, UK*

<sup>4</sup>*Department of Physics, Lund Institute of Technology, PO Box 118, SE-221 00 Lund, Sweden*

<sup>5</sup>*Physique Atomique et Astrophysique, Université de Mons – UMONS, 20 Place du Parc, B-7000 Mons, Belgium*

<sup>6</sup>*IPNAS, Université de Liège, B15 Sart Tilman, B-4000 Liège, Belgium*

Accepted 2017 August 18. Received 2017 August 18; in original form 2017 July 12

## ABSTRACT

The lifetimes of 17 even-parity levels (3d5s, 3d4d, 3d6s, and 4p<sup>2</sup>) in the region 57743–77837 cm<sup>−1</sup> of singly ionised scandium (Sc II) were measured by two-step time-resolved laser induced fluorescence spectroscopy. Oscillator strengths of 57 lines from these highly excited upper levels were derived using a hollow cathode discharge lamp and a Fourier transform spectrometer. In addition, Hartree–Fock calculations where both the main relativistic and core-polarisation effects were taken into account were carried out for both low- and high-excitation levels. There is a good agreement for most of the lines between our calculated branching fractions and the measurements of [Lawler and Dakin \(1989\)](#) in the region 9000–45000 cm<sup>−1</sup> for low excitation levels and with our measurements for high excitation levels in the region 23500–63100 cm<sup>−1</sup>. This, in turn, allowed us to combine the calculated branching fractions with the available experimental lifetimes to determine semi-empirical oscillator strengths for a set of 380 E1 transitions in Sc II. These oscillator strengths include the weak lines that were used previously to derive the solar abundance of scandium. The solar abundance of scandium is now estimated to  $\log \epsilon_{\odot} = 3.04 \pm 0.13$  using these semi-empirical oscillator strengths to shift the values determined by [Scott et al. \(2015\)](#). The new estimated abundance value is in agreement with the meteoritic value ( $\log \epsilon_{\text{met}} = 3.05 \pm 0.02$ ) of [Lodders et al. \(2009\)](#).

**Key words:** atomic data – methods: laboratory: atomic – methods: numerical – Sun: abundances – techniques: spectroscopic

## 1 INTRODUCTION

The iron-group elements ( $21 \leq Z \leq 28$ ) are produced during supernova type Ia explosions, while supernova type II explosions are responsible for the formation of  $\alpha$ -elements such as Mg, Si, S. The even-Z nuclei such as S, Ca, Ti, Cr, and Fe have higher cosmic abundance compared to the odd-Z nuclei located in between because of the consecutive capture of  $\alpha$ -particles. The production of odd-Z elements is not as well understood, and does not follow the abundance trends of the  $\alpha$ -elements, indicating non-common production mechanisms. In recent years, this has caused an increasing interest

in the odd-Z iron-peak elements in astrophysics. Abundance determinations in stars constrain the stellar evolution and supernova explosion models ([Pagel 2009](#)). Moreover, transitions from highly excited levels have additional diagnostic value, since they can be used to benchmark non local thermodynamical equilibrium (NLTE) modelling of stellar atmospheres. Besides the development of 3D hydrodynamic model atmospheres, a trustworthy NLTE treatment is the current challenge for accurate stellar abundances. High-precision atomic data for selected lines are important for this development ([Lind et al. 2012](#)).

In the case of scandium ( $Z = 21$ ), a realistic 3D NLTE solar atmosphere model has been used by [Scott et al. \(2015\)](#) to revise the solar abundance of scandium resulting in a photospheric value in significant disagreement with the me-

<sup>★</sup> E-mail: asli.pehlivan@mah.se (APR)

<sup>†</sup> E-mail: patrick.palmeri@umons.ac.be (PP)

teoritic abundance (Lodders et al. 2009). Scott et al. (2015) used experimental transition probabilities of five Sc I and nine Sc II lines determined by Lawler and Dakin (1989). The latter authors combined their measured branching fractions with the time-resolved laser induced fluorescence (TR-LIF) lifetimes of Marsden et al. (1988) to obtain absolute  $A$ -values for transitions depopulating 51 levels in Sc I and 18 levels in Sc II. In Marsden et al. (1988), only three highly-excited even-parity levels of Sc II, belonging to  $3d4d\ ^3G$ , were measured. Older lifetime measurements in singly ionised scandium have focussed on lower excited odd-parity  $3d4p$  and  $4s4p$  levels (Buchta et al. 1971; Arnesen et al. 1976; Palenius et al. 1976; Vogel et al. 1985). On the theoretical side, the most recent calculations of E1 oscillator strengths in Sc II are Ruczkowski et al. (2014) and Kurucz (2011).

The main goal of the present work is to provide a new set of experimental  $f$ -values for transitions depopulating the highly-excited even-parity levels in Sc II, and new calculations for both low- and high-excitation levels and lines. Descriptions of our measurements are presented in Section 2 and 3. The theoretical method used for the calculation of the radiative parameters is described in Section 4. In Section 5, our results are presented and compared to data available in the literature. The consequence of the proposed set of oscillator strengths on the solar abundance of scandium is discussed in Section 6. Finally, our conclusions are given in Section 7.

## 2 LIFETIME MEASUREMENTS

The experimental set-up for the two-step Time-Resolved Laser Induced Fluorescence (TR-LIF) measurements at the Lund High Power Laser Facility has been described in detail by Engström et al. (2014) and Lundberg et al. (2016). For an overview we refer to Figure 1 in Lundberg et al. (2016), and here we give only the most important details. A frequency doubled Nd:YAG laser (Continuum Surelite) with 10 ns pulses was used to produce the free scandium ions by focusing the light on a rotating solid scandium sample in a vacuum chamber with a pressure around  $10^{-4}$  mbar. The ions in the plasma cone were crossed by two laser beams, a few mm above the solid sample, generating the two-step excitations. The fluorescence signal was detected in a direction perpendicular to both the ablation and excitation lasers.

For the first step ( $4s-4p$ ), we used a Continuum Nd - 60 dye laser with either DCM or Pyridine 2 dyes. The 10 ns long pulses were frequency doubled using a KDP crystal, giving the wavelengths needed for the first step. The second laser system excited the final high energy levels. It consists of a frequency doubled Continuum NY-82 Nd:YAG laser pumping a Continuum Nd - 60 dye laser with either DCM or Oxacin dye for wavelengths below or above 660 nm, respectively. The pulse length was reduced from 10 ns to less than one ns by stimulated Brillouin scattering. The output was frequency doubled using a KDP crystal and, where higher energy was needed, tripled with a BBO crystal.

For two step excitation, the timing between the pulses is crucial. For this purpose, a delay generator ensures that the second step is timed to when the population of the intermediate state is at its flat maximum as determined by observing the decay of this level in another channel, see Fig-

ure 2 in Lundberg et al. (2016).

The fluorescence emitted by the scandium ions was filtered by a 1/8 m grating monochromator with its 0.28 mm wide entrance slit oriented parallel to the excitation laser beams. This fluorescence light was recorded using a fast micro-channel-plate photomultiplier tube (Hamamatsu R3809U) and digitised using a Tektronix DPO 7254 oscilloscope with 2.5 GHz analog bandwidth. We used the second spectral order with a 0.5 nm observed line width for all measurements. The excitation laser pulse shape was recorded simultaneously using a fast photo diode and digitised by another channel of the oscilloscope. All decay curves were averaged over 1000 laser pulses and analysed using the DECFIT software (Palmeri et al. 2008) by fitting a single exponential function convoluted by the measured shape of the second-step laser pulse and a background function to the observed decay.

The excitation schemes of the measured Sc II levels are presented in Table 1. This table shows the intermediate levels and their excitation wavelengths, the final levels and their excitation wavelengths from the intermediate levels together with the detection channel level and wavelength. For the levels  $4d\ ^3S_1$ ,  $4d\ ^1D_2$  and  $4p^2\ ^3P_2$ , it was possible to record the decay in more than one channel. We did not find any differences in the lifetimes obtained from the different channels. Sc II is a complex spectrum with a dense level structure, as shown in Figure 1. Line blending can be caused by cascades or fluorescence from the intermediate level as discussed by Lundberg et al. (2016). For all measurements, we investigated if there was a line blend affecting the recorded curves. Due to the small spectral width of the laser compared to the energy level separations, we avoid exciting multiple levels.

To investigate any possible saturation effects in the second step excitation, a set of neutral density filters was placed in the excitation beam. The delay between the ablation and first excitation pulse, the geometrical alignment of the lasers in respect to the target as well as the intensity of the ablation laser were varied to test time-of-flight effects. No systematic effects were observed.

As discussed in Palmeri et al. (2008), the weighting of individual data points, hence the purely statistical uncertainty in the fitted lifetime, is difficult to estimate accurately because the digitising process is not strictly a counting measurement. However, extensive tests have shown that even for weak lines the dominating factor is the variation between different measurements. The uncertainty in Table 2 represents the uncertainty of 10-20 measurements performed over several days. The difference between subsequent curves is significantly lower than the quoted uncertainty, usually less than 1%.

## 3 BRANCHING FRACTION MEASUREMENTS

A water-cooled hollow cathode discharge lamp (HCL) was used to produce the free scandium ions. The lamp has an iron cathode with anodes on each side, separated by glass cylinders. A small piece of scandium was placed in the cathode. We used argon, with a pressure of 0.3 Torr, as a buffer gas and applied currents ranging from 0.2 to 0.5 A. These measurements at different currents are very important to find

and compensate for self-absorption effects. If self-absorption is not treated correctly, the measured relative line intensity may be less than the true intensity of the line. This in turn changes the branching fraction which is essential to derive oscillator strengths. Self-absorption was observed in the case of the  $3d4d\ ^3D_3$ ,  $3d4d\ ^3S_1$ , and  $3d4d\ ^3P_2$  levels, and the affected lines were corrected. More details on this procedure can be found in [Pehlivan et al. \(2015\)](#).

The spectra were recorded with the vacuum ultraviolet Fourier transform spectrometer (VUV FTS) at the Blackett Laboratory, Imperial College London ([Pickering, J.C. 2002](#)) in the interval  $23500 - 63100\ \text{cm}^{-1}$  ( $425 - 158\ \text{nm}$ ) using a resolution of  $0.039\ \text{cm}^{-1}$ . We used two different photomultiplier tube detectors: Hamamatsu R7154 and R11568, the latter with a UG5 filter. Each scandium measurement consists of 12 co-added scans. To determine the relative response functions of the system, we used standard lamps: a tungsten filament lamp ( $800 - 300\ \text{nm}$ ) and a deuterium lamp ( $410 - 116\ \text{nm}$ ) for the wavelength region ( $425 - 210\ \text{nm}$ ), and a deuterium standard lamp alone for the region ( $317 - 158\ \text{nm}$ ). The tungsten lamp was calibrated by the UK National Physical Laboratory and the deuterium lamp by Physikalisch-Technische Bundesanstalt, in Berlin. In the region where the lamps overlap, the response functions were placed on the same relative scale. We recorded the spectrum of the calibration lamps immediately before and after each scandium measurement. The HCL and the calibration lamps were placed at the same distances from the FTS, and a mirror was used to select the light source without moving the lamps.

In astrophysics, oscillator strengths ( $f$ -values) or  $\log(gf)$  values are the parameters used for abundance analysis. The  $f$ -value is proportional to the transition probability for E1 transitions by

$$f = \frac{g_u}{g_l} \lambda^2 A_{ul} 1.499 \times 10^{-16}, \quad (1)$$

where  $g_u$  is the statistical weight of the upper level,  $g_l$  the statistical weight of the lower level,  $\lambda$  the wavelength of the transition in Å, and  $A_{ul}$  the transition probability in  $\text{s}^{-1}$ .

The transition probability is related to the branching fraction ( $BF$ ) and the lifetime of the upper level ( $\tau_u$ ). It can be derived using

$$A_{ul} = \frac{BF_{ul}}{\tau_u}. \quad (2)$$

We obtained the lifetimes of the upper levels from our measurements, as discussed in Section 2. The  $BF$  is the parameter we measure and it is defined as the transition probability of the line,  $A_{ul}$ , divided by the sum of transition probabilities of all lines from the same upper level;

$$BF_{ul} = \frac{A_{ul}}{\sum_i A_{ui}} = \frac{I_{ul}}{\sum_i I_{ui}}. \quad (3)$$

Since all lines emanate from the same upper level, the transition probability is proportional to the line intensity,  $I_{ul}$ , which for FTS spectra is proportional to photon flux ([Davis S.P. et al. 2001](#)). Therefore, we derived  $BF$ s from calibrated intensity ratios in our measurements. All lines were identified using the analysis of [Johansson and Litzén \(1980\)](#). The intensities of the observed lines were determined by fitting Gaussian line profiles using GFit ([Engström 1998, 2014](#)).

The uncertainty of the  $A$ -value, and thus of the  $f$ -value,

arises from the uncertainty in the upper level lifetime and the uncertainty of the  $BF$ . The latter includes the uncertainty in the intensity calibration procedure and the uncertainty in the measured line intensity, including the self-absorption correction. The uncertainties of the integrated line intensities were determined using GFit. The relative uncertainties are as low as 0.1% for strong lines and 4% on average. However, for two weak lines the uncertainty is as large as 20%. The uncertainty in the calibration using the tungsten lamp is 2.2% and the uncertainty using the deuterium lamp is 8.6% for the region  $425 - 210\ \text{nm}$  and 9.9% between  $317$  and  $158\ \text{nm}$ . These calibration lamp uncertainties include the calibration uncertainty and the variation resulting from the repeated measurements made before and after all scandium scans. The uncertainties of the radiative lifetimes are given in Table 2. Finally, we were not able to observe the weakest lines from the investigated level. However, we included their contributions as residuals with derived theoretical  $BF$ s from our calculations. The residual  $BF$ s are less than 7% for all levels. The uncertainties in the residuals were estimated to 50% and included in the error budget. The final uncertainties in the oscillator strengths are presented in Table 3 and were derived from the individual contributions using the method described by [Sikström et al. \(2002\)](#).

#### 4 RADIATIVE PARAMETER CALCULATIONS

To calculate branching fractions and the oscillator strengths in Sc II, we used the relativistic Hartree–Fock (HFR) method implemented in the Cowan’s suite of atomic structure computer codes ([Cowan 1981](#)). It is modified by including a pseudo-potential and a correction to the electric dipole operator that take into account the core-polarisation effects giving rise to the HFR+CPOL technique ([Quinet et al. 1999](#)).

In this study, the valence-valence correlation was included using the following configuration interaction (CI) expansions:  $3d4s + 3d5s + 3d6s + 3d7s + 3d^2 + 3d4d + 3d5d + 3d6d + 3d7d + 3d5g + 3d6g + 3d7g + 4s^2 + 4s5s + 4s6s + 4s7s + 4s4d + 4s5d + 4s6d + 4s7d + 4s5g + 4s6g + 4s7g + 4p^2 + 4d^2 + 4f^2 + 4p4f$  for the even parity;  $3d4p + 3d5p + 3d6p + 3d7p + 3d4f + 3d5f + 3d6f + 3d7f + 3d6h + 3d7h + 4s4p + 4s5p + 4s6p + 4s7p + 4s4f + 4s5f + 4s6f + 4s7f + 4s6h + 4s7h + 4p4d + 4d4f$  for the odd parity.

Regarding the core-polarisation effects, a Sc IV  $3p^6$  closed-subshell ionic core was considered where the dipole polarisability,  $\alpha_d = 2.129\ a_0^3$  was taken from the RRPA calculations of [Johnson et al. \(1983\)](#) and a cut-off radius of  $1.17\ a_0$  was estimated as the HFR mean radius of the outermost  $3p$  orbital,  $\langle 3p|r|3p \rangle_{\text{HFR}}$ .

During a least-squares-fit procedure, we adjusted some radial integrals to minimise the discrepancies between the hamiltonian eigenvalues and the experimental energy levels taken from the NIST Atomic Spectra Database ([Kramida et al. 2015](#)). The latter are based on the term analysis originally carried out by [Russell and Meggers \(1927\)](#) and later revised by [Neufeld \(1970\)](#) and by [Johansson and Litzén \(1980\)](#). There are 168 levels belonging to the configurations  $3d4s$ ,  $3d^2$ ,  $3d4p$ ,  $4s4p$ ,  $3d5s$ ,  $3d4d$ ,  $3d5p$ ,  $4p^2$ ,  $3d4f$ ,  $3d6s$ ,  $4s5s$ ,  $3d5d$ ,  $4s4d$ ,  $3d5f$ ,  $3d5g$ ,  $3d7s$ ,  $3d6d$ , and  $3d6f$ . The average energies,  $E_{\text{av}}$ , of the above-mentioned known configurations along with their direct,  $F^k$ , exchange,  $G^k$ , electrostatic and

spin-orbit,  $\zeta$ , radial parameters were considered in the fit of the energy levels. The *ab initio* and fitted parameter values are reported in Tables 4 and 5 for the even and odd configurations, respectively. The spin-orbit integrals not presented in these tables were fixed to their HFR+CPOL values. The other Slater integrals, including the CI  $R^k$  parameters, not reported here, were fixed to 80% of their *ab initio* values to account for missing CI effects (Cowan 1981). The average deviations of the least-squares-fits were  $157 \text{ cm}^{-1}$  for the 93 even-parity experimental levels and  $65 \text{ cm}^{-1}$  for the 75 odd-parity experimental levels.

## 5 RESULTS AND DISCUSSION

Table 2 compares our TR-LIF and HFR+CPOL lifetimes with other experimental values from the literature (Buchta et al. 1971; Arnesen et al. 1976; Palenius et al. 1976; Vogel et al. 1985; Marsden et al. 1988), the Hartree-Fock values calculated by Kurucz (2011) and the lifetimes deduced from the semi-empirical oscillator strengths calculated by Ruczkowski et al. (2014). On average, our HFR+CPOL lifetimes are shorter than the measurements for the odd-parity levels and longer for the even-parity levels. The discrepancies range from a few percent to about 20%, except for the even-parity levels  $4p^2 \ ^1D_2$  and  $3d6s \ ^3D_3$  where they reach 57% and 49%, respectively. In the former case, this state is strongly mixed (our calculation gives 36%  $4p^2 \ ^1D_2$  + 36%  $4s4d \ ^1D_2$  + 23%  $3d6s \ ^1D_2$ ) and an important decay channel ( $4p^2 \ ^1D_2 \rightarrow 3d4p \ ^1D_2$   $BF = 0.0713$ ) is affected by cancellation (the cancellation factor as defined by Cowan (1981) is less than 5%) that could explain the over estimated lifetime. Concerning  $3d6s \ ^3D_3$  level, no such argument could explain the observed disagreement. The beam-foil measurements of Buchta et al. (1971) can be rejected for the levels  $3d4p \ ^3D_3, \ ^1P_1^o, \ ^1F_3^o$  as previously stated by Marsden et al. (1988) due to blending problems.

The calculations by Kurucz (2011) show roughly the same systematic discrepancy with experiment (lifetimes shorter for the odd parity and longer for the even parity) as our HFR+CPOL calculations. Although the calculation of Kurucz (2011) shows a better agreement than HFR+CPOL for certain  $3d4d$  levels ( $^3F_{2,4}, \ ^1D_2, \ ^3P_2$ ), it does not solve the theory-experiment disagreements observed for the levels  $4p^2 \ ^1D_2$  and  $3d6s \ ^3D_3$ . The parametric calculation of Ruczkowski et al. (2014) agrees with our HFR+CPOL model within 10% including all levels. Unfortunately, no lifetime value can be deduced from Ruczkowski et al. (2014) for the levels  $4p^2 \ ^1D_2$  and  $3d6s \ ^3D_3$ . Concerning the level  $3d4d \ ^3G_3$ , our TR-LIF measurement is slightly lower than the one of Marsden et al. (1988) although the error bars do overlap.

For all  $3d4p$  levels, our HFR+CPOL model and the parametric calculation of Ruczkowski et al. (2014) are closer to the measurement of Marsden et al. (1988). The excellent agreement between Marsden et al. (1988) and Ruczkowski et al. (2014) is not surprising as the latter adjusted the dipole transition integrals to the oscillator strengths determined from the branching fraction measurements of Lawler and Dakin (1989) combined with the lifetime measurements of Marsden et al. (1988). For most of the higher levels, the lifetimes calculated by Kurucz (2011) are closer to our measurements than those of Ruczkowski et al. (2014).

Although there is a systematic discrepancy between the theoretical and experimental lifetimes, we find a better agreement when comparing our calculated  $BF$ s with the experimental values. For the high excitation lines, measured in this work, the averaged  $BF$  ratio is  $1.02 \pm 0.16$  with respect to the calculated values. Similarly, Figure 2 shows the good agreement between  $BF$ s computed in this study using the HFR+CPOL method and the measurements by Lawler and Dakin (1989). Here, the averaged  $BF$  ratio is  $0.98 \pm 0.20$ . Based on these comparisons, the calculated  $BF$ s were combined with our TR-LIF lifetimes and those of Marsden et al. (1988) to determine rescaled transition probabilities and oscillator strengths.

In Table 3, we present our experimental  $\log(gf)$  values, together with the measured  $BF$ s, the uncertainties and the corresponding rescaled theoretical oscillator strengths,  $\log(gf)_{\text{resc}}$ . Figure 3 illustrates the final agreement between our experimental  $\log(gf)$  values and the calculated  $\log(gf)_{\text{resc}}$ . Table 6 summarises our calculated radiative parameters along with the weighted transition probabilities ( $gA$ ), the weighted oscillator strengths in the log scale ( $\log(gf)$ ), the HFR+CPOL branching fractions ( $BF$ ), and the cancellation factor ( $CF$ ) as defined by Cowan (1981).

Our rescaled theoretical oscillator strengths are compared to the semi-empirical values calculated by Ruczkowski et al. (2014) in Figure 4. As expected, the scatter increases for the weak lines, i.e. the transitions with  $\log(gf) \lesssim -1$ , where cancellation effects could be an issue. For instance, the transition  $3d4p \ ^3P_2^o - 4p^2 \ ^3P_2$  labelled in Table 6 76589(e)2 – 29824(o)2 has a very low cancellation factor ( $CF = 0.001$ ) that indicates a strong cancellation effect in our HFR+CPOL line strength calculation. Indeed, the rescaled oscillator strength for that transition is  $\log(gf)_{\text{resc}} = -2.83$  which is three orders of magnitude lower (in the linear scale) than the value predicted by Ruczkowski et al. (2014) ( $\log(gf) = -0.02$ ). On the other hand, a transition for which the cancellation effects in our model is not an issue ( $CF > 0.05$ ) such as  $3d4p \ ^3F_3^o - 3d4d \ ^3F_4$  (63529(e)4 – 27602(o)3) has an oscillator strength predicted by Ruczkowski et al. (2014) ( $\log(gf) = -3.35$ ) that is two orders of magnitude lower than our rescaled value ( $\log(gf)_{\text{resc}} = -1.44$ ). This could indicate a strong cancellation effect in their calculation. Unfortunately, they did not estimate any cancellation factors. For the strongest transitions, i.e.  $\log(gf) \gtrsim -1$ , the mean scatter drops to about 20% in the linear scale.

In Figure 5, our semi-empirical values are compared to the calculation of Kurucz (2011) where a similar global correlation is observed. The mean scatter in this case is also found to be  $\sim 20\%$  for transitions with  $\log(gf) \gtrsim -1$  and increases for weaker lines. Here again, the cancellation factors are not available in Kurucz's database (Kurucz 2011). But, for example, our predicted strong line  $3d5p \ ^3F_3^o - 3d6s \ ^3D_3$  (77387(e)3 – 66564(o)3) with  $\log(gf)_{\text{resc}} = 0.16$  and  $CF = 0.379$  is certainly affected by a strong cancellation effect in the calculation of Kurucz (2011) dramatically lowering its oscillator strength to  $\log(gf) = -2.56$ .

Based on the differences between different sets of  $BF$ s discussed above and including the uncertainties of the experimental lifetimes, we estimate the accuracy of the rescaled theoretical  $f$ -values to be 10% for the strong lines and 15 – 20% for other lines.

## 6 CONSEQUENCE ON THE SOLAR ABUNDANCE OF SCANDIUM

Scott et al. (2015) have redetermined the solar abundances of the iron-peak elements employing a 3D model atmosphere that takes into account departures from the local thermodynamic equilibrium. However, the significant discrepancy between the photospheric and the meteoritic abundances (Lodders et al. 2009) still remains for scandium with  $\log \epsilon_{\odot} = 3.16 \pm 0.04$  and  $\log \epsilon_{\text{met}} = 3.05 \pm 0.02$ .

The Sc II lines used in Scott et al. (2015) for the determination of the solar abundance of scandium are presented in Table 7. These lines are from low-excited levels measured by Lawler and Dakin (1989) but not included in our present study. The third column of this table contains the oscillator strengths deduced from the  $A$ -values of Lawler and Dakin (1989) used by Scott et al. (2015) to determine the photospheric abundances listed in sixth column. They are compared to our rescaled oscillator strengths reported in the fourth column and the differences between the two values are given in the log scale in the fifth column. For this set of solar lines, our oscillator strengths are systematically larger than those of Lawler and Dakin (1989) by  $\sim 0.1$  dex on average, if we exclude the transition  $3d^2 \ ^1D_2 - 3d4p \ ^1D_2^{\circ}$  for which our  $f$ -value is affected by strong cancellation effects. Column seven in Table 7 gives the abundances obtained from each line, assuming they are all lying on the linear part of the curve of growth (see the upper left panel of Figure 3 in Scott et al. (2015)), with our new  $gf$ -values.

The weighted average along with the corresponding weighted standard deviation of the abundance were determined using the weights of Scott et al. (2015), reported in the last column of Table 7. Their weights range from one to three and are based on the line quality for abundance determination. Discarding the line  $3d^2 \ ^1D_2 - 3d4p \ ^1D_2^{\circ}$  from the mean estimate, one obtains  $\log \epsilon_{\text{cor}} = 3.04 \pm 0.13$  (where the second number is the standard deviation) for the corrected photospheric abundance, now in good agreement with the meteoritic value of Lodders et al. (2009). Even if we reject the transition  $3d^2 \ ^3F_4 - 3d4p \ ^3F_3^{\circ}$  for which there is a factor of two difference between our rescaled  $f$ -value and the experimental value of Lawler and Dakin (1989), the mean  $\log \epsilon_{\text{cor}} = 3.10 \pm 0.05$  is still in accord with the meteoritic value. Moreover, considering the full line set does not change the agreement ( $\log \epsilon_{\text{cor}} = 3.07 \pm 0.17$ ). Finally we note that, all these weighted average abundances agree within the mutual error bars with the value determined by Scott et al. (2015) using only Sc I lines ( $\log \epsilon = 3.14 \pm 0.09$ ).

Replacing our  $f$ -value set by the one of Kurucz (2011) will not change this accord either ( $\log \epsilon_{\text{kur}} = 3.10 \pm 0.09$ ). This is not the case for the set of Ruczkowski et al. (2014). Indeed, the photospheric abundance would be estimated significantly too high with respect to the meteoritic value, i.e.  $\log \epsilon_{\text{ruc}} = 3.44 \pm 0.31$ . Even if the transition  $3d^2 \ ^3F_4 - 3d4p \ ^3F_3^{\circ}$  for which the oscillator strength calculated by Ruczkowski et al. (2014) ( $\log(gf)_{\text{ruc}} = -3.28$ ) is one order of magnitude lower than the experimental value of Lawler and Dakin (1989) is excluded, this would not significantly improve the situation ( $\log \epsilon_{\text{ruc}} = 3.29 \pm 0.01$ ).

It should be noted, however, that the lines used for these studies are weak, see Figure 6. Their  $BF$ s are less than 5% except for  $\lambda 566.904$  having  $\sim 10\%$ . These small  $BF$ s make it

difficult to measure and calculate with high accuracy. The real uncertainty might thus be larger than the observed scatter.

## 7 CONCLUSIONS

New TR-LIF lifetimes were measured using two-step excitation schemes in Sc II. These measurements extend the set of available experimental values with 17 even-parity levels belonging to the excited configurations  $3d5s$ ,  $3d4d$ ,  $4p^2$  and  $3d6s$ . We measured 57  $BF$ s from these upper levels using a HCL and a FTS. By combining the  $BF$ s with the measured lifetimes, we derived  $\log(gf)$  values from these highly-excited levels. A Hartree-Fock model that includes the main relativistic interactions along with the core-polarisation effects (HFR+CPOL) was used to determine the branching fractions and the oscillator strengths. The comparison between our HFR+CPOL and TR-LIF lifetimes along with those found in the literature (Buchta et al. 1971; Arnesen et al. 1976; Palenius et al. 1976; Vogel et al. 1985; Marsden et al. 1988; Ruczkowski et al. 2014; Kurucz 2011) shows generally a good agreement ranging from a few percent to 20% with the notable exceptions of the even-parity levels  $4p^2 \ ^1D_2$  and  $3d6s \ ^3D_3$ . The former discrepancy may be due to a cancellation effect that lengthens the HFR+CPOL lifetime. Owing to the good agreement ( $\sim 20\%$ ) obtained with the experimental branching fractions of Lawler and Dakin (1989) for low-excitation levels and ours for high-excitation levels, the HFR+CPOL branching fractions were combined with our TR-LIF lifetimes and the experimental values of Marsden et al. (1988) to obtain rescaled semi-empirical oscillator strengths for all the 380 E1 transitions depopulating the 34 fine-structure levels for which TR-LIF lifetimes are available. This new set of oscillator strengths were compared to the parametric calculation of Ruczkowski et al. (2014) and to the Hartree-Fock values of Kurucz (2011). In both cases, the mean scatters were  $\sim 20\%$  for the strong lines ( $\log(gf) \gtrsim -1$ ) giving an estimate of the accuracy for these radiative parameters. Finally, the solar abundance of scandium was estimated to  $\log \epsilon_{\odot} = 3.04 \pm 0.13$  using our rescaled semi-empirical oscillator strengths to correct the values determined in the recent study of Scott et al. (2015). This value is in improved agreement with the meteoritic value ( $\log \epsilon_{\text{met}} = 3.05 \pm 0.02$ ) of Lodders et al. (2009).

## ACKNOWLEDGEMENTS

This work was financially supported by the Integrated Initiative of Infrastructure Project LASERLAB-EUROPE, contract LLC002130, and the Belgian FRS-FNRS. PQ and PP are, respectively Research Director and Research Associate of the FRS-FNRS. We acknowledge the support from the Swedish Research Council through a Linnaeus grant to the Lund Laser Centre and through project grant 2016-04185, as well as the Knut and Alice Wallenberg Foundation. MTB, JCP, and CC thank the STFC (UK) for support of their Laboratory Astrophysics research at Imperial College London. VF is currently a post-doctoral researcher of the Return Grant programme of the Belgian Scientific Policy (BEL-SPO). The Belgian team is grateful to the Swedish colleagues

for the warm hospitality enjoyed at the Lund Laser Centre during the two campaigns of measurements performed in June and August 2015.

## REFERENCES

- Arnesen A., Bengtsson B., Curtis L. J., Hallin R., Nordling C., Noreland T., 1976, *Phys. Lett.*, 56A, 355
- Buchta R., Curtis L. J., Martinson I., Brzozowski J., 1971, *Phys. Scr.*, 4, 55
- Casey A. R., Schlaufman K. C., 2015, *ApJ*, 809, 13
- Cowan R. D., 1981, *The Theory of Atomic Structure and Spectra* (Berkeley, CA: University of California Press)
- Davis, S.P., Abrams M.C., and Brault J.W. (2001) *Fourier Transform Spectrometry*. San Diego : Academic Press (section 1.4)
- Engström L., 1998, GFit, A Computer Program to Determine Peak Positions and Intensities in Experimental Spectra (Tech. Rep. LRAP-232, Atomic Physics, Lund University)
- Engström L., 2014, GFit, <http://kurslab-atom.fysik.lth.se/Lars/GFit/Html/index.html>,
- Engström L., Lundberg H., Nilsson H., Hartmann H., Bäckström E., 2014, *Astron. Astrophys.*, 570, A34
- Johansson S., Litzén U., 1980, *Phys. Scr.*, 22, 49
- Johnson W. R., Kolb D., Huang K.-N., 1983, *Atom. Dat. Nucl. Dat. Tables*, 28, 333
- Kramida A., Ralchenko Yu., Reader J., and NIST ASD Team, 2015, *NIST Atomic Spectra Database (ver. 5.2)* [Online]. Available: <http://physics.nist.gov/asd> [2015, August 17]
- Kurucz R. L., 2011, [Online]. Available: <http://kurucz.harvard.edu/atoms.html> [2015, August 17]
- Lind K., Bergmann M., Asplund M., 2012, *MNRAS*, 427, 50
- Lodders K., Palme H., Gail H.-P., 2009, *Landolt Börnstein, New Series, Vol. VI/4B, Chap. 4.4, Abundances of the Elements in the Solar System*, ed. J. E. Trümper (Springer-Verlag, Berlin), 560-630
- Lundberg H., Hartman H., Engström L., Nilsson H., Palmeri P., Quinet P., Fivet V., Malcheva G., Blagoev K., 2016, *MNRAS*, 460, 356
- Lawler J. E., Dakin J. T., 1989, *J. Opt. Soc. Am. B*, 6, 1457
- Marsden G. C., Den Hartog E. A., Lawler J. E., Dakin J. T., Roberts V. D., 1988, *J. Opt. Soc. Am. B*, 5, 606
- Neufeld L. W., 1970, *Dissertation, Kansas State University*
- Pagel E. B. J., 2009, *Nucleosynthesis and Chemical Evolution of Galaxies* (Cambridge University Press)
- Palenius H. P., Curtis L. J., Lundlin L., 1976, *J. Phys. B*, 9, L473
- Palmeri P., Quinet P., Fivet V., Biémont E., Nilsson H., Engström L., Lundberg H., 2008, *Phys. Scr.*, 78, 015304
- Pehlivan A., Nilsson H., Hartman, H., 2015, *A&A*, 582, A98
- Pickering, J.C., 2002, *Vibrational Spectroscopy*, 29(1,2), 27
- Quinet P., Palmeri P., Biémont E., McCurdy M. M., Rieger G., Pinnington E. H., Wickliffe M. E., Lawler J. E., 1999, *Mon. Not. R. Astr. Soc.*, 307, 934
- Ruczkowski J., Elantkowska M., Dembczynski J., 2014, *J.Q.S.R.T.*, 145, 20
- Russell H. N., Meggers W. F., 1927, *Sci. Papers Natl. Bur. Stand. (U.S.)*, 22, 329
- Scott P., Asplund M., Grevesse N., Bergemann M., Sauval A. J., 2015, *A&A*, 573, A26
- Sikström C. M., Nilsson, H., Litzen, U., Blom, A., Lundberg, H. 2002, *J. Quant. Spectr. Rad. Transf.*, 74, 355
- Vogel O., Ward L., Arnesen A., Hallin R., Nordling C., Wannstrom A., 1985, *Phys. Scr.*, 31, 166

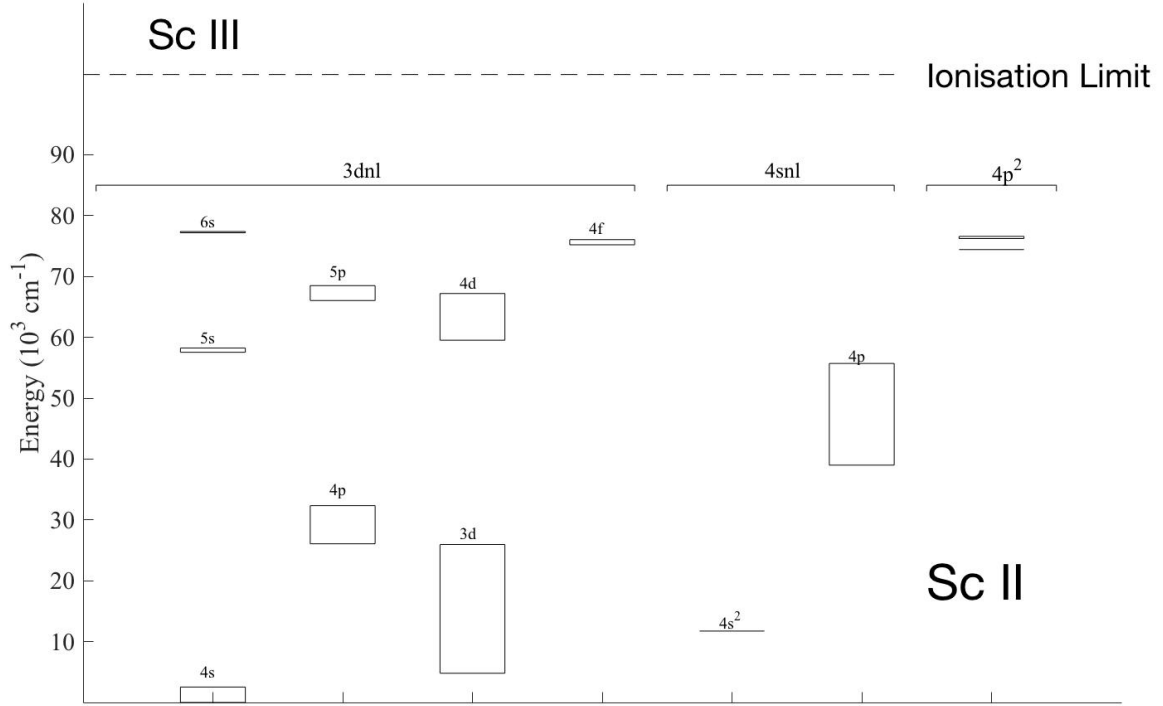


**Figure 1.** Partial energy level diagram of Sc II, the energy level values are from [Johansson and Litzén \(1980\)](#). Each box consists of several levels.

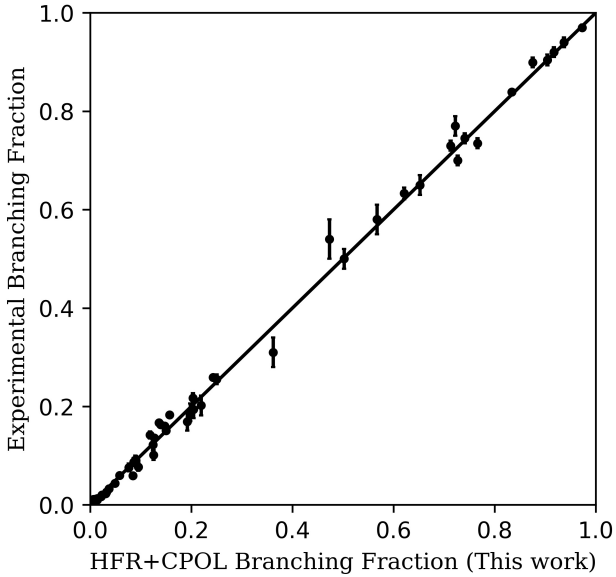


**Figure 2.** Comparison between the HFR+CPOL branching fractions of this work and the experimental values of [Lawler and Dakin \(1989\)](#). The straight line of equality has been drawn.

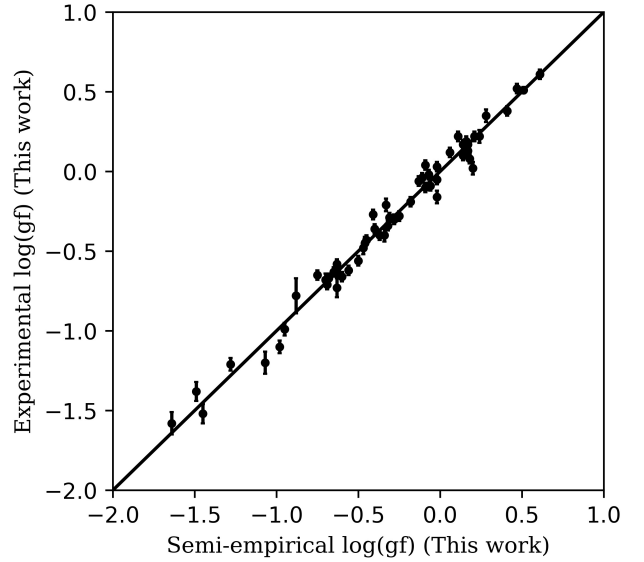


**Figure 3.** Comparison between the oscillator strengths determined by the combination of the HFR+CPOL branching fractions and the TR-LIF lifetimes of this work and the experimental oscillator strengths derived in this work. The straight line of equality has been drawn.

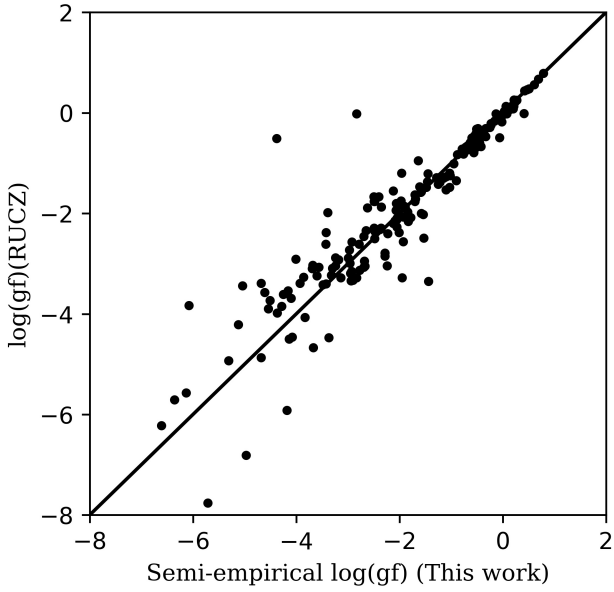


**Figure 4.** Comparison between the oscillator strengths determined by the combination of the HFR+CPOL branching fractions and the TR-LIF lifetimes (This Work) and the semi-empirical oscillator strengths calculated by [Ruczkowski et al. \(2014\)](#) (RUCZ). The straight line of equality has been drawn.

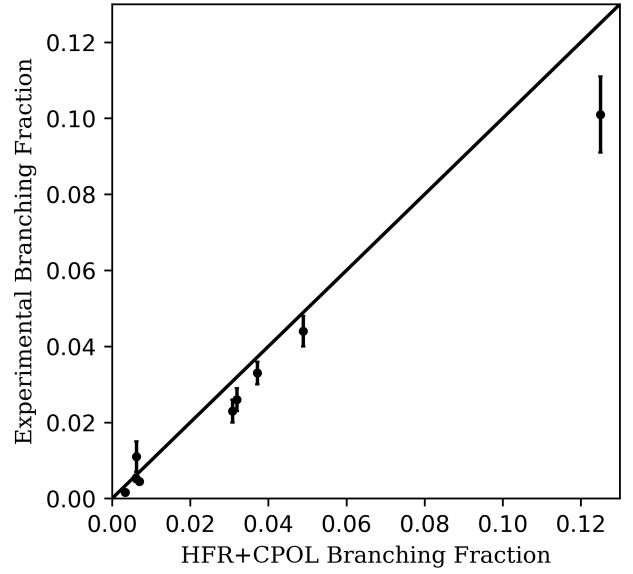


**Figure 6.** Comparison between the HFR+CPOL branching fractions and the experimental values of [Lawler and Dakin \(1989\)](#) for the Sc II lines used in the determination of the solar scandium abundance. The straight line of equality has been drawn.

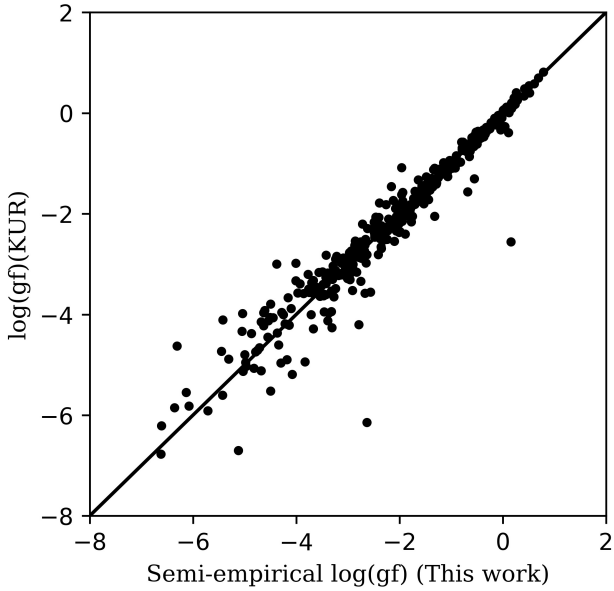


**Figure 5.** Comparison between the oscillator strengths determined by the combination of the HFR+CPOL branching fractions and the TR-LIF lifetimes (This Work) and the oscillator strengths calculated by [Kurucz \(2011\)](#) (KUR). The straight line of equality has been drawn.



**Table 1.** Measured Sc II levels and the corresponding two-step excitation schemes

Final Level <sup>a</sup>	First Step Excitation		Second Step Excitation		Detection		
	Starting Level <sup>a</sup> (cm <sup>-1</sup> )	Intermediate Level <sup>a</sup> (cm <sup>-1</sup> )	$\lambda_{air}$ (nm)	Final Level <sup>a</sup> (cm <sup>-1</sup> )	$\lambda_{air}$ (nm)	Lower Level <sup>a</sup> (cm <sup>-1</sup> )	$\lambda_{air}$ (nm)
5s <sup>3</sup> D <sub>3</sub>	67.72	27602.45	363.07	57743.92	331.67	27841.35	334.32
5s <sup>1</sup> D <sub>2</sub>	67.72	27602.45	363.07	58252.09	326.17	32349.98	385.96
4d <sup>1</sup> F <sub>3</sub>	177.76	29823.93	337.22	59528.42	336.55	26081.34	298.89
4d <sup>3</sup> D <sub>1</sub>	177.76	29823.93	337.22	59875.08	332.67	27917.78	312.83
4d <sup>3</sup> D <sub>2</sub>	177.76	29823.93	337.22	59929.46	332.07	28021.29	313.31
4d <sup>3</sup> D <sub>3</sub>	177.76	29823.93	337.22	60001.91	331.27	28161.17	313.97
4d <sup>3</sup> G <sub>3</sub>	177.76	29823.93	337.22	60267.16	328.39	27443.71	304.57
4d <sup>1</sup> P <sub>1</sub>	177.76	29823.93	337.22	60400.41	326.95	26081.34	291.30
4d <sup>3</sup> S <sub>1</sub>	177.76	29823.93	337.22	61071.43	319.93	29823.93	319.93
						39345.52	460.15
4d <sup>3</sup> F <sub>2</sub>	2540.95	32349.98	335.37	63374.63	322.23	27917.78	281.95
4d <sup>3</sup> F <sub>4</sub>	2540.95	32349.98	335.37	63528.54	320.64	28161.17	282.66
4d <sup>1</sup> D <sub>2</sub>	2540.95	32349.98	335.37	64366.68	312.25	26081.34	261.12
						30815.70	297.97
4d <sup>3</sup> P <sub>2</sub>	2540.95	32349.98	335.37	64705.89	308.98	29823.93	286.60
4p <sup>2</sup> <sup>1</sup> D <sub>2</sub>	177.76	28161.17	357.25	74433.30	216.04	32349.98	237.55
4p <sup>2</sup> <sup>3</sup> P <sub>1</sub>	177.76	29823.93	337.22	76360.80	214.82	39345.52	270.08
4p <sup>2</sup> <sup>3</sup> P <sub>2</sub>	177.76	29823.93	337.22	76589.30	213.76	28161.17	206.43
						39115.04	266.77
						39345.52	268.42
6s <sup>3</sup> D <sub>3</sub>	177.76	29823.93	337.22	77387.17	210.18	28161.17	203.08

<sup>a</sup> All energy level values and wavelength values are from [Johansson and Litzén \(1980\)](#).<sup>b</sup> 2 $\omega$  and 3 $\omega$  stand for, respectively, frequency doubling and tripling excitation schemes. All first step levels are excited using a frequency doubling scheme (2 $\omega$ )

**Table 2.** Comparison of radiative lifetimes ( $\tau$ ) in Sc II

Level <sup>a</sup>	$E^a$ (cm <sup>-1</sup> )	$\tau_{\text{this cal}}^b$ (ns)	$\tau_{\text{this exp}}^c$ (ns)	$\tau_{\text{other exp}}$ (ns)	$\tau_{\text{other cal}}$ (ns)
3d4p <sup>1</sup> D <sub>2</sub> <sup>o</sup>	26081.34	6.65		7.5±0.4 <sup>d</sup> 7.16±0.18 <sup>e</sup> 7.8±0.8 <sup>h</sup>	6.54 <sup>i</sup> 7.79 <sup>j</sup>
3d4p <sup>3</sup> F <sub>2</sub> <sup>o</sup>	27443.71	5.68		6.2±0.3 <sup>d</sup> 6.2±0.2 <sup>f</sup> 6.5±0.4 <sup>g</sup>	5.38 <sup>i</sup> 5.90 <sup>j</sup>
3d4p <sup>3</sup> F <sub>3</sub> <sup>o</sup>	27602.45	5.62		6.1±0.3 <sup>d</sup>	5.32 <sup>i</sup> 5.83 <sup>j</sup>
3d4p <sup>3</sup> F <sub>4</sub> <sup>o</sup>	27841.35	5.54		5.6±0.6 <sup>h</sup>	5.24 <sup>i</sup> 5.75 <sup>j</sup>
3d4p <sup>3</sup> D <sub>1</sub> <sup>o</sup>	27917.78	4.44		4.7±0.2 <sup>d</sup> 4.61±0.10 <sup>e</sup>	4.20 <sup>i</sup> 4.67 <sup>j</sup>
3d4p <sup>3</sup> D <sub>2</sub> <sup>o</sup>	28021.29	4.41		4.7±0.2 <sup>d</sup> 4.66±0.14 <sup>e</sup>	4.17 <sup>i</sup> 4.64 <sup>j</sup>
3d4p <sup>3</sup> D <sub>3</sub> <sup>o</sup>	28161.17	4.38		4.7±0.2 <sup>d</sup> 4.55±0.15 <sup>e</sup> 6.1±0.6 <sup>h</sup>	4.15 <sup>i</sup> 4.59 <sup>j</sup>
3d4p <sup>3</sup> P <sub>0</sub> <sup>o</sup>	29736.27	6.36		7.7±0.4 <sup>d</sup> 7.48±0.18 <sup>e</sup>	6.80 <sup>i</sup> 7.44 <sup>j</sup>
3d4p <sup>3</sup> P <sub>1</sub> <sup>o</sup>	29742.16	6.39		7.6±0.4 <sup>d</sup> 7.3±0.3 <sup>e</sup>	6.76 <sup>i</sup> 7.45 <sup>j</sup>
3d4p <sup>3</sup> P <sub>2</sub> <sup>o</sup>	29823.93	6.30		7.4±0.4 <sup>d</sup> 7.30±0.16 <sup>e</sup>	6.67 <sup>i</sup> 7.50 <sup>j</sup>
3d4p <sup>1</sup> P <sub>1</sub> <sup>o</sup>	30815.70	8.10		8.8±0.4 <sup>d</sup> 8.5±0.6 <sup>g</sup> 5.5±0.5 <sup>h</sup>	7.35 <sup>i</sup> 8.76 <sup>j</sup>
3d4p <sup>1</sup> F <sub>3</sub> <sup>o</sup>	32349.98	4.68		5.1±0.3 <sup>d</sup> 5.2±0.2 <sup>e</sup> 6.8±0.6 <sup>h</sup>	4.46 <sup>i</sup> 5.20 <sup>j</sup>
4s4p <sup>3</sup> P <sub>0</sub> <sup>o</sup>	39002.20	3.69		3.7±0.2 <sup>d</sup>	3.36 <sup>i</sup> 3.66 <sup>j</sup>
4s4p <sup>3</sup> P <sub>1</sub> <sup>o</sup>	39115.04	3.69		3.7±0.2 <sup>d</sup>	3.37 <sup>i</sup> 3.67 <sup>j</sup>
4s4p <sup>3</sup> P <sub>2</sub> <sup>o</sup>	39345.52	3.70		3.8±0.2 <sup>d</sup>	3.39 <sup>i</sup> 3.67 <sup>j</sup>
4s4p <sup>1</sup> P <sub>1</sub> <sup>o</sup>	55715.36	0.88			0.91 <sup>i</sup>
3d5s <sup>3</sup> D <sub>1</sub>	57551.88	3.49			3.44 <sup>i</sup>
3d5s <sup>3</sup> D <sub>2</sub>	57614.40	3.50			3.44 <sup>i</sup>
3d5s <sup>3</sup> D <sub>3</sub>	57743.92	3.50	3.20±0.20		3.44 <sup>i</sup>
3d5s <sup>1</sup> D <sub>2</sub>	58252.09	3.70	3.26±0.20		3.66 <sup>j</sup>
3d4d <sup>1</sup> F <sub>3</sub>	59528.42	2.69	2.32±0.15		2.51 <sup>i</sup> 2.51 <sup>j</sup>

Table 2. Continued.

Level <sup>a</sup>	$E^a$ ( $\text{cm}^{-1}$ )	$\tau_{\text{this cal}}^b$ (ns)	$\tau_{\text{this exp}}^c$ (ns)	$\tau_{\text{other exp}}$ (ns)	$\tau_{\text{other cal}}$ (ns)
3d4d <sup>3</sup> D <sub>1</sub>	59875.08	2.72	2.23±0.15		2.62 <sup>i</sup>
3d4d <sup>3</sup> D <sub>2</sub>	59929.46	2.74	2.32±0.15		2.63 <sup>i</sup>
3d4d <sup>3</sup> D <sub>3</sub>	60001.91	2.76	2.41±0.20		2.58 <sup>j</sup>
3d4d <sup>3</sup> G <sub>3</sub>	60267.16	2.50	2.19±0.15	2.5±0.2 <sup>d</sup>	2.65 <sup>i</sup>
3d4d <sup>3</sup> G <sub>4</sub>	60348.46	2.52		2.4±0.2 <sup>d</sup>	2.33 <sup>i</sup>
3d4d <sup>1</sup> P <sub>1</sub>	60400.41	2.89	2.44±0.15		2.47 <sup>j</sup>
3d4d <sup>3</sup> G <sub>5</sub>	60457.12	2.54		2.5±0.2 <sup>d</sup>	2.35 <sup>i</sup>
3d4d <sup>3</sup> S <sub>1</sub>	61071.43	2.82	2.45±0.15		2.49 <sup>j</sup>
3d4d <sup>3</sup> F <sub>2</sub>	63374.63	2.40	2.15±0.10		2.69 <sup>i</sup>
3d4d <sup>3</sup> F <sub>3</sub>	63445.16	2.41			2.63 <sup>j</sup>
3d4d <sup>3</sup> F <sub>4</sub>	63528.54	2.43	2.19±0.10		2.38 <sup>i</sup>
3d4d <sup>1</sup> D <sub>2</sub>	64366.68	2.73	2.25±0.15		2.51 <sup>j</sup>
3d4d <sup>3</sup> P <sub>0</sub>	64615.77	3.21			2.77 <sup>i</sup>
3d4d <sup>3</sup> P <sub>1</sub>	64646.70	3.21			2.78 <sup>j</sup>
3d4d <sup>3</sup> P <sub>2</sub>	64705.89	3.19	2.51±0.15		2.05 <sup>i</sup>
3d4d <sup>1</sup> G <sub>4</sub>	65236.04	3.17			2.43 <sup>j</sup>
3d4d <sup>1</sup> S <sub>0</sub>	67216.56	3.87			2.05 <sup>i</sup>
4p <sup>2</sup> <sup>1</sup> D <sub>2</sub>	74433.30	5.96	3.80±0.15		2.47 <sup>j</sup>
4p <sup>2</sup> <sup>3</sup> P <sub>0</sub>	76243.20	1.17			2.26 <sup>i</sup>
4p <sup>2</sup> <sup>3</sup> P <sub>1</sub>	76360.80	1.17	1.14±0.06		2.65 <sup>i</sup>
4p <sup>2</sup> <sup>3</sup> P <sub>2</sub>	76589.30	1.18	1.09±0.06		2.65 <sup>i</sup>
3d6s <sup>3</sup> D <sub>1</sub>	77195.19	5.56			2.45 <sup>i</sup>
3d6s <sup>3</sup> D <sub>2</sub>	77256.99	5.55			2.74 <sup>i</sup>
3d6s <sup>3</sup> D <sub>3</sub>	77387.17	5.54	3.73±0.25		6.80 <sup>i</sup>
3d6s <sup>1</sup> D <sub>2</sub>	77833.88	6.61			1.28 <sup>i</sup>

<sup>a</sup> Johansson and Litzén (1980).<sup>b</sup> HFR+CPOL calculation. This work.<sup>c</sup> TR-LIF measurements. This work.<sup>d</sup> TR-LIF measurements by Marsden et al. (1988).<sup>e</sup> TR-LIF measurements by Vogel et al. (1985).<sup>f</sup> TR-LIF measurements by Arnesen et al. (1976).<sup>g</sup> Beam-foil spectroscopy by Palenius et al. (1976).<sup>h</sup> Beam-foil spectroscopy by Buchta et al. (1971).<sup>i</sup> Hartree-Fock calculation by Kurucz (2011).<sup>j</sup> Parametric method calculation by Ruczkowski et al. (2014).

**Table 3.** Presentation of experimental  $\log(gf)$  values together with the transition, wavelength,  $\lambda$ , wavenumber,  $\sigma$ , measured branching fraction,  $BF_{\text{exp}}$ , experimental transition probability,  $A_{\text{exp}}$ , and the corresponding rescaled semi-empirical  $\log(gf)$  values of this work. The radiative lifetimes,  $\tau$ , are TR-LIF measurements from this work.

Config.	Upper level <sup>a</sup> Energy (cm <sup>-1</sup> )	Lower level <sup>a</sup> Energy (cm <sup>-1</sup> )	Config.	$\lambda_{\text{exp}}$ (nm)	$\sigma_{\text{exp}}$ (cm <sup>-1</sup> )	$\sigma_{\text{theo}}^b$ (cm <sup>-1</sup> )	$BF_{\text{exp}}$	$BF$ unc. %	$A_{\text{exp}}$ (s <sup>-1</sup> )	$\log(gf)$ Exp.	$\log(gf)_{\text{resc}}$ Calc.
3d5s <sup>3</sup> D <sub>3</sub> $\tau = 3.20 \pm 0.20$ ns	57744	3d4p <sup>3</sup> F <sub>3</sub> <sup>o</sup>	331.673	30141.50	30176	6.21E-02	4	1.94E+07	-0.65±0.03	-0.75	
		3d4p <sup>3</sup> F <sub>2</sub> <sup>o</sup>	334.323	29902.57	29944	4.05E-01	3	1.27E+08	0.17±0.03	0.14	
		3d4p <sup>3</sup> D <sub>2</sub> <sup>o</sup>	336.347	29722.58	29771	5.29E-02	4	1.65E+07	-0.71±0.03	-0.69	
		3d4p <sup>3</sup> D <sub>3</sub> <sup>o</sup>	337.938	29582.76	29620	3.60E-01	3	1.12E+08	0.13±0.03	0.17	
		3d4p <sup>3</sup> P <sub>2</sub> <sup>o</sup>	358.064	27919.88	27888	1.20E-01	4	3.75E+07	-0.30±0.03	-0.28	
		<i>Residual</i>				3.37E-03					
3d5s <sup>1</sup> D <sub>2</sub> $\tau = 3.26 \pm 0.20$ ns	58252	3d4p <sup>1</sup> D <sub>2</sub> <sup>o</sup>	310.751	32179.68	32040	4.90E-01	2	1.50E+08	0.04±0.03	-0.09	
		3d4p <sup>3</sup> F <sub>2</sub> <sup>o</sup>	324.493	30808.34	30866	1.08E-02	16	3.30E+06	-1.58±0.07	-1.64	
		3d4p <sup>1</sup> P <sub>1</sub> <sup>o</sup>	364.376	27436.43	27508	1.48E-01	4	4.55E+07	-0.34±0.03	-0.32	
		3d4p <sup>1</sup> F <sub>3</sub> <sup>o</sup>	385.960	25902.13	25865	3.51E-01	5	1.08E+08	0.08±0.03	0.18	
				<i>Residual</i>				2.10E-02			
3d4d <sup>1</sup> F <sub>3</sub> $\tau = 2.32 \pm 0.15$ ns	59528	3d4p <sup>1</sup> D <sub>2</sub> <sup>o</sup>	298.893	33447.17	33296	8.22E-01	0.5	3.54E+08	0.52±0.03	0.47	
		3d4p <sup>3</sup> D <sub>2</sub> <sup>o</sup>	318.712	31367.21	31408	6.54E-03	14	2.82E+06	-1.52±0.06	-1.45	
		3d4p <sup>1</sup> F <sub>3</sub> <sup>o</sup>	367.834	27178.50	27121	1.72E-01	7	7.40E+07	0.02±0.04	0.20	
				<i>Residual</i>				5.10E-03			
3d4d <sup>3</sup> D <sub>1</sub> $\tau = 2.23 \pm 0.15$ ns	59875	3d4p <sup>3</sup> F <sub>2</sub> <sup>o</sup>	308.254	32431.14	32475	1.22E-01	5	5.49E+07	-0.63±0.04	-0.63	
		3d4p <sup>3</sup> D <sub>1</sub> <sup>o</sup>	312.827	31957.28	32026	4.57E-01	3	2.05E+08	-0.04±0.03	-0.11	
		3d4p <sup>3</sup> D <sub>2</sub> <sup>o</sup>	313.843	31853.76	31913	1.17E-01	5	5.24E+07	-0.63±0.04	-0.65	
		3d4p <sup>3</sup> P <sub>0</sub> <sup>o</sup>	331.703	30138.84	30134	1.79E-01	4	8.02E+07	-0.40±0.03	-0.37	
		3d4p <sup>3</sup> P <sub>1</sub> <sup>o</sup>	331.768	30132.91	30123	1.25E-01	5	5.61E+07	-0.56±0.04	-0.50	
		<i>Residual</i>				3.75E-02					
3d4d <sup>3</sup> D <sub>2</sub> $\tau = 2.32 \pm 0.15$ ns	59929	3d4p <sup>3</sup> F <sub>3</sub> <sup>o</sup>	309.249	32327.05	32372	1.21E-01	5	5.23E+07	-0.43±0.03	-0.45	
		3d4p <sup>3</sup> D <sub>1</sub> <sup>o</sup>	312.296	32011.74	32081	8.39E-02	5	3.62E+07	-0.58±0.03	-0.63	
		3d4p <sup>3</sup> D <sub>2</sub> <sup>o</sup>	313.309	31908.30	31968	4.12E-01	3	1.78E+08	0.12±0.03	0.06	
		3d4p <sup>3</sup> D <sub>3</sub> <sup>o</sup>	314.688	31768.28	31816	6.61E-02	5	2.85E+07	-0.67±0.03	-0.68	
		3d4p <sup>3</sup> P <sub>0</sub> <sup>o</sup>	331.170	30187.30	30178	2.50E-01	4	1.08E+08	-0.05±0.03	-0.02	
		<i>Residual</i>				6.67E-02					
						3.42E-02					
3d4d <sup>3</sup> D <sub>3</sub> $\tau = 2.41 \pm 0.20$ ns	60002	3d4p <sup>3</sup> F <sub>4</sub> <sup>o</sup>	310.850	32160.62	32214	9.39E-02	6	3.90E+07	-0.40±0.04	-0.34	
		3d4p <sup>3</sup> D <sub>2</sub> <sup>o</sup>	312.599	31980.37	32041	4.35E-02	7	1.81E+07	-0.73±0.06	-0.63	
		3d4p <sup>3</sup> D <sub>3</sub> <sup>o</sup>	313.972	31840.77	31890	5.16E-01	4	2.14E+08	0.35±0.04	0.28	
		3d4p <sup>3</sup> P <sub>0</sub> <sup>o</sup>	331.272	30178.03	30157	3.47E-01	5	1.44E+08	0.22±0.04	0.24	
				<i>Residual</i>				3.51E-02			

Table 3. Continued.

Config.	Upper level <sup>a</sup> Energy (cm <sup>-1</sup> )	Lower level <sup>a</sup> Energy (cm <sup>-1</sup> )	$\lambda_{\text{exp}}^a$ (nm)	$\sigma_{\text{exp}}^a$ (cm <sup>-1</sup> )	$\sigma_{\text{theo}}^b$ (cm <sup>-1</sup> )	$BF_{\text{exp}}$	$BF$ unc. %	$A_{\text{exp}}$ (s <sup>-1</sup> )	$\log(gf)_{\text{Exp.}}$	$\log(gf)_{\text{resc}}$ Calc.
3d4d <sup>3</sup> G <sub>3</sub> $\tau = 2.19 \pm 0.15$ ns	60267	3d4p <sup>3</sup> F <sub>2</sub> <sup>o</sup>	304.572	32823.36	32822	9.26E-01	1	4.23E+08	0.61±0.03	0.61
		3d4p <sup>3</sup> F <sub>3</sub> <sup>o</sup>	306.052	32664.51	32664	7.41E-02	8	3.38E+07	-0.48±0.04	-0.47
		<i>Residual</i>				6.20E-03				
3d4d <sup>1</sup> P <sub>1</sub> $\tau = 2.44 \pm 0.15$ ns	60400	3d4p <sup>1</sup> D <sub>2</sub> <sup>o</sup>	291.298	34319.09	34206	3.98E-01	7	1.63E+08	-0.21±0.04	-0.33
		3d4p <sup>1</sup> P <sub>1</sub> <sup>o</sup>	337.915	29584.65	29673	6.02E-01	5	2.47E+08	0.10±0.03	0.14
		<i>Residual</i>				7.27E-02				
3d4d <sup>3</sup> S <sub>1</sub> $\tau = 2.45 \pm 0.15$ ns	61071	3d4p <sup>3</sup> P <sub>0</sub> <sup>o</sup>	319.038	31335.12	31336	1.13E-01	7	4.60E+07	-0.68±0.04	-0.70
		3d4p <sup>3</sup> P <sub>1</sub> <sup>o</sup>	319.098	31329.24	31326	2.84E-01	6	1.16E+08	-0.28±0.04	-0.25
		3d4p <sup>3</sup> P <sub>2</sub> <sup>o</sup>	319.933	31247.50	31231	5.73E-01	4	2.34E+08	0.03±0.03	-0.02
		3d4p <sup>1</sup> P <sub>2</sub> <sup>o</sup>	330.421	30255.76	30319	3.04E-02	10	1.24E+07	-1.21±0.05	-1.28
		<i>Residual</i>				6.10E-02				
3d4d <sup>3</sup> F <sub>2</sub> $\tau = 2.15 \pm 0.10$ ns	63375	3d4p <sup>3</sup> F <sub>2</sub> <sup>o</sup>	278.230	35930.81	35960	3.57E-01	5	1.66E+08	-0.02±0.03	-0.07
		3d4p <sup>3</sup> F <sub>3</sub> <sup>o</sup>	279.464	35772.19	35802	3.72E-02	9	1.73E+07	-0.99±0.04	-0.95
		3d4p <sup>3</sup> D <sub>1</sub> <sup>o</sup>	281.950	35456.96	35511	5.27E-01	3	2.45E+08	0.17±0.02	0.17
		3d4p <sup>3</sup> D <sub>2</sub> <sup>o</sup>	282.776	35353.30	35398	7.88E-02	6	3.66E+07	-0.66±0.03	-0.60
		<i>Residual</i>				1.59E-02				
3d4d <sup>3</sup> F <sub>4</sub> $\tau = 2.19 \pm 0.10$ ns	63529	3d4p <sup>3</sup> F <sub>2</sub> <sup>o</sup>	280.130	35687.12	35726	3.42E-01	6	1.56E+08	0.22±0.03	0.21
		3d4p <sup>3</sup> D <sub>3</sub> <sup>o</sup>	282.663	35367.30	35402	6.58E-01	3	3.01E+08	0.51±0.02	0.51
		<i>Residual</i>				8.18E-03				
3d4d <sup>1</sup> D <sub>2</sub> $\tau = 2.25 \pm 0.15$ ns	64367	3d4p <sup>1</sup> D <sub>2</sub> <sup>o</sup>	261.119	38285.22	38187	7.25E-01	4	3.22E+08	0.22±0.03	0.11
		3d4p <sup>3</sup> F <sub>2</sub> <sup>o</sup>	270.754	36923.00	37012	1.69E-02	12	7.51E+06	-1.38±0.06	-1.49
		3d4p <sup>3</sup> P <sub>1</sub> <sup>o</sup>	288.728	34624.48	34661	2.27E-02	16	1.01E+07	-1.20±0.07	-1.07
		3d4p <sup>1</sup> P <sub>1</sub> <sup>o</sup>	297.967	33550.90	33654	2.35E-01	8	1.05E+08	-0.16±0.04	-0.02
		<i>Residual</i>				4.94E-02				
3d4d <sup>3</sup> P <sub>2</sub> $\tau = 2.51 \pm 0.15$ ns	64706	3d4p <sup>3</sup> D <sub>3</sub> <sup>o</sup>	273.556	36544.66	36597	1.59E-01	8	6.32E+07	-0.45±0.04	-0.46
		3d4p <sup>3</sup> P <sub>1</sub> <sup>o</sup>	285.927	34963.68	34960	1.78E-01	6	7.09E+07	-0.36±0.04	-0.40
		3d4p <sup>3</sup> P <sub>2</sub> <sup>o</sup>	286.597	34881.86	34865	6.33E-01	3	2.52E+08	0.19±0.03	0.16
		3d4p <sup>1</sup> P <sub>1</sub> <sup>o</sup>	294.984	33890.19	33953	3.08E-02	8	1.23E+07	-1.10±0.04	-0.98
		<i>Residual</i>				4.86E-02				
4p <sup>2</sup> <sup>3</sup> P <sub>1</sub> $\tau = 1.14 \pm 0.06$ ns	76361	3d4p <sup>3</sup> D <sub>2</sub> <sup>o</sup>	206.804	48339.50	48384	3.16E-01	7	2.77E+08	-0.27±0.04	-0.41
		4s4p <sup>3</sup> P <sub>0</sub> <sup>o</sup>	267.597	37358.69	37358	2.29E-01	6	2.01E+08	-0.19±0.03	-0.18
		4s4p <sup>3</sup> P <sub>1</sub> <sup>o</sup>	268.407	37245.53	37245	1.80E-01	6	1.58E+08	-0.29±0.03	-0.31
		4s4p <sup>3</sup> P <sub>2</sub> <sup>o</sup>	270.079	37014.70	37014	2.75E-01	6	2.41E+08	-0.10±0.03	-0.09
<i>Residual</i>				6.46E-02						

**Table 3.** Continued.

Config.	Upper level <sup>a</sup> Energy (cm <sup>-1</sup> )	Lower level <sup>a</sup> Energy (cm <sup>-1</sup> )	$\lambda_{\text{exp}}^a$ (nm)	$\sigma_{\text{exp}}^a$ (cm <sup>-1</sup> )	$\sigma_{\text{theo}}^b$ (cm <sup>-1</sup> )	$BF_{\text{exp}}$	$BF$ unc. %	$A_{\text{exp}}$ (s <sup>-1</sup> )	$\log(gf)_{\text{Exp.}}$	$\log(gf)_{\text{Calc.}}$
4p <sup>2</sup> 3P <sub>2</sub>	76589	28021	205.831	48568.03	48615	5.63E-02	27	5.17E+07	-0.78±0.11	-0.88
$\tau = 1.09 \pm 0.06$ ns		28161	206.426	48428.15	48464	2.95E-01	6	2.71E+08	-0.06±0.03	-0.13
		39115	266.771	37474.35	37477	1.65E-01	6	1.52E+08	-0.09±0.03	-0.06
		39346	268.422	37243.72	37246	4.83E-01	4	4.43E+08	0.38±0.03	0.41
		<i>Residual</i>				1.18E-02				

<sup>a</sup> Energy level, wavelength, and wavenumber values are taken from [Johansson and Litzén \(1980\)](#) which are available in NIST database ([Kramida et al. 2015](#)).

<sup>b</sup> Theoretical wavenumber values are from the calculations of this work.

**Table 4.** Radial parameters adopted in the HFR+CPOL calculations for the even-parity configurations of Sc II. The parameters not listed here have been fixed to their *ab initio* values or to 80% of their HFR+CPOL values for the electrostatic integrals.

Config.	Parameter	<i>Ab initio</i> (cm <sup>-1</sup> )	Fitted (cm <sup>-1</sup> )	Ratio	Note <sup>a</sup>
3d4s	$E_{av}$	1075	1137		
	$\zeta_{3d}$	83	72	0.87	
	$G^2(3d4s)$	11351	9883	0.87	
3d5s	$E_{av}$	57881	58144		
	$\zeta_{3d}$	87	79	0.91	
	$G^2(3d5s)$	2071	1851	0.89	
3d6s	$E_{av}$	77397	77497		
	$\zeta_{3d}$	88	82	0.93	
	$G^2(3d6s)$	789	631	0.80	F
3d7s	$E_{av}$	86487	86549		
	$\zeta_{3d}$	88	69	0.78	
	$G^2(3d7s)$	393	314	0.80	F
3d <sup>2</sup>	$E_{av}$	11721	9531		
	$F^2(3d3d)$	49657	37346	0.75	
	$F^4(3d3d)$	30556	22011	0.72	
	$\alpha$	0	64		
	$\beta$	0	-962		
	$T$	0	3		
	$\zeta_{3d}$	65	59	0.91	
3d4d	$E_{av}$	62210	62852		
	$\zeta_{3d}$	87	79	0.91	
	$\zeta_{4d}$	8	8	1.00	F
	$F^2(3d4d)$	7539	5977	0.79	
	$F^4(3d4d)$	3599	2816	0.78	
	$G^0(3d4d)$	6862	2467	0.36	
	$G^2(3d4d)$	4352	3238	0.74	
	$G^4(3d4d)$	2927	2327	0.80	
3d5d	$E_{av}$	79393	79170		
	$\zeta_{3d}$	87	86	0.99	
	$\zeta_{5d}$	3	3	1.00	F
	$F^2(3d5d)$	2896	2158	0.75	
	$F^4(3d5d)$	1388	1099	0.79	
	$G^0(3d5d)$	2416	1008	0.42	R
	$G^2(3d5d)$	1640	684	0.42	R
	$G^4(3d5d)$	1122	469	0.42	R
3d6d	$E_{av}$	87550	87894		
	$\zeta_{3d}$	88	88	1.00	F
	$\zeta_{6d}$	2	2	1.00	F
	$F^2(3d6d)$	1458	1166	0.80	F
	$F^4(3d6d)$	705	564	0.80	F
	$G^0(3d6d)$	1176	941	0.80	F
	$G^2(3d6d)$	822	658	0.80	F
	$G^4(3d6d)$	571	454	0.80	F
3d5g	$E_{av}$	85492	85761		
	$\zeta_{3d}$	88	78	0.89	
	$\zeta_{5g}$	0	0	1.00	F
	$F^2(3d5g)$	465	420	0.90	
	$F^4(3d5g)$	42	34	0.81	
	$G^2(3d5g)$	6	5	0.80	F
	$G^4(3d5g)$	4	3	0.80	F
	$G^6(3d5g)$	2	2	0.80	F

**Table 4.** Continued.

Config.	Parameter	<i>Ab initio</i> (cm <sup>-1</sup> )	Fitted (cm <sup>-1</sup> )	Ratio	Note <sup>a</sup>
4s <sup>2</sup>	$E_{av}$	16845	16876		
4s5s	$E_{av}$	78974	79141		
	$G^0(4s5s)$	2341	1765	0.75	
4s4d	$E_{av}$	83034	82930		
	$\zeta_{4d}$	9	9	1.00	F
	$G^2(4s4d)$	6830	5464	0.80	F
4p <sup>2</sup>	$E_{av}$	77789	80625		
	$F^2(4p4p)$	28516	29802	1.05	
	$\zeta_{4p}$	199	253	1.27	

<sup>a</sup> F and R stand for, respectively, a fixed parameter value and a fixed ratio between these parameters.

**Table 5.** Radial parameters adopted in the HFR+CPOL calculations for the odd-parity configurations of Sc II. The parameters not listed here have been fixed to their *ab initio* values or to 80% of their HFR+CPOL values for the electrostatic integrals.

Config.	Parameter	<i>Ab initio</i> (cm <sup>-1</sup> )	Fitted (cm <sup>-1</sup> )	Ratio	Note <sup>a</sup>
3d4p	$E_{av}$	28207	28996		
	$\zeta_{3d}$	85	91	1.07	
	$\zeta_{4p}$	146	162	1.11	
	$F^2(3d4p)$	14647	12024	0.82	
	$G^1(3d4p)$	6709	6289	0.94	
3d5p	$G^3(3d4p)$	5361	4338	0.81	
	$E_{av}$	66759	66915		
	$\zeta_{3d}$	87	73	0.84	
	$\zeta_{5p}$	50	50	1.00	F
	$F^2(3d5p)$	4168	3375	0.81	
	$G^1(3d5p)$	1560	1397	0.90	
3d4f	$G^3(3d5p)$	1380	900	0.65	
	$E_{av}$	75021	75609		
	$\zeta_{3d}$	88	74	0.84	
	$\zeta_{4f}$	0	0	1.00	F
	$F^2(3d4f)$	2127	1766	0.83	
	$F^4(3d4f)$	514	367	0.71	
	$G^1(3d4f)$	420	354	0.84	
	$G^3(3d4f)$	242	194	0.80	F
3d5f	$G^5(3d4f)$	166	133	0.80	F
	$E_{av}$	85220	85564		
	$\zeta_{3d}$	88	91	1.03	
	$\zeta_{5f}$	0	0	1.00	F
	$F^2(3d5f)$	1051	841	0.80	F
	$F^4(3d5f)$	296	238	0.80	F
	$G^1(3d5f)$	289	232	0.80	F
	$G^3(3d5f)$	168	135	0.80	F
	$G^5(3d5f)$	116	93	0.80	F
3d6f	$E_{av}$	90728	91031		
	$\zeta_{3d}$	88	88	1.00	F
	$\zeta_{6f}$	0	0	1.00	F
	$F^2(3d6f)$	597	478	0.80	F
	$F^4(3d6f)$	181	145	0.80	F
	$G^1(3d6f)$	188	151	0.80	F
	$G^3(3d6f)$	111	88	0.80	F
	$G^5(3d6f)$	76	61	0.80	F
4s4p	$E_{av}$	41287	43719		
	$\zeta_{4p}$	197	242	1.23	
	$G^1(4s4p)$	37326	27686	0.74	

<sup>a</sup> F stands for a fixed parameter value.



**Table 6.** Calculated branching fractions ( $BF$ ), oscillator strengths ( $\log(gf)$ ), oscillator strengths ( $\log(gf)_{\text{resc}}$ ) along with the corresponding scaled values ( $\log(gf)_{\text{resc}}$ ;  $gA_{\text{resc}}$ ) in Sc II. Only the transitions depopulating the levels for which the lifetime has been measured are listed. The experimental lifetimes ( $\tau_u$ ) used to scale the  $f$ - and  $A$ -values are also reported.

Upper level <sup>a</sup>	$\tau_u$ (ns)	Lower level <sup>a</sup>	$\lambda^b$ (nm)	$BF$	$gA$ (s <sup>-1</sup> )	$gA_{\text{resc}}$ (s <sup>-1</sup> )	$\log(gf)$	$\log(gf)_{\text{resc}}$	CF <sup>c</sup>					
26081	(o) 2	7.5 <sup>d</sup>	0	(e) 1	383.307	5.91E-03	4.44E+06	-2.01	-2.06	0.468				
			68	(e) 2	384.305	1.40E-02	1.05E+07	-1.64	-1.69	0.927				
			178	(e) 3	385.938	1.65E-05	1.24E+04	-4.56	-4.61	0.006				
			2541	(e) 2	424.682	9.73E-01	7.31E+08	6.49E+08	0.29	0.24	0.975			
			4803	(e) 2	469.827	7.55E-04	5.67E+05	5.03E+05	-2.73	-2.78	0.260			
			4884	(e) 3	471.616	3.77E-05	2.83E+04	2.51E+04	-4.03	-4.08	0.047			
			10945	(e) 2	660.460	6.19E-03	4.65E+06	4.13E+06	-1.53	-1.57	0.036			
			12102	(e) 1	715.119	6.88E-07	5.17E+02	4.59E+02	-5.41	-5.45	0.009			
			12154	(e) 2	717.836	8.89E-06	6.68E+03	5.93E+03	-4.30	-4.34	0.008			
			27444	(o) 2	6.2 <sup>d</sup>	0	(e) 1	364.278	7.27E-01	6.40E+08	0.11	0.07	0.888	
						68	(e) 2	365.180	1.57E-01	1.38E+08	-0.56	-0.60	0.894	
						178	(e) 3	366.653	6.61E-03	5.82E+06	5.33E+06	-1.93	-1.97	0.927
2541	(e) 2	401.448				1.27E-02	1.12E+07	1.03E+07	-1.57	-1.61	0.837			
4803	(e) 2	441.556				8.94E-02	7.87E+07	7.21E+07	-0.64	-0.68	0.971			
4884	(e) 3	443.135				7.01E-03	6.17E+06	5.65E+06	-1.74	-1.78	0.466			
10945	(e) 2	605.924				1.13E-04	9.98E+04	9.15E+04	-3.26	-3.30	0.046			
12102	(e) 1	651.617				2.08E-05	1.83E+04	1.68E+04	-3.93	-3.97	0.676			
12154	(e) 2	653.872				2.60E-06	2.29E+03	2.10E+03	-4.83	-4.87	0.053			
27602	(o) 3	6.1 <sup>d</sup>				68	(e) 2	363.074	7.66E-01	9.54E+08	0.28	0.24	0.871	
						178	(e) 3	364.531	1.36E-01	1.69E+08	-0.47	-0.51	0.952	
						2541	(e) 2	398.906	7.51E-04	9.35E+05	8.62E+05	-2.65	-2.69	0.768
			4803	(e) 2	438.481	7.95E-03	9.90E+06	9.12E+06	-1.54	-1.58	0.966			
			4884	(e) 3	440.039	8.59E-02	1.07E+08	9.86E+07	-0.51	-0.54	0.975			
			4988	(e) 4	442.067	3.37E-03	4.20E+06	3.87E+06	-1.91	-1.95	0.242			
			10945	(e) 2	600.150	4.67E-06	5.82E+03	5.36E+03	-4.50	-4.54	0.520			
			12154	(e) 2	647.153	4.47E-05	5.57E+04	5.13E+04	-3.46	-3.49	0.612			
			14261	(e) 4	749.355	5.08E-08	6.33E+01	5.83E+01	-6.28	-6.31	0.089			
			27841	(o) 4	6.1 <sup>d</sup>	178	(e) 3	361.383	9.04E-01	1.47E+09	0.46	0.42	0.949	
						4884	(e) 3	435.460	6.12E-03	9.96E+06	9.03E+06	-1.55	-1.59	0.976
						4988	(e) 4	437.446	9.04E-02	1.47E+08	1.33E+08	-0.37	-0.42	0.976
14261	(e) 4	736.173				7.87E-07	1.28E+03	1.16E+03	-4.99	-5.03	0.912			
27918	(o) 1	4.7 <sup>d</sup>				0	(e) 1	358.092	5.67E-01	3.83E+08	-0.13	-0.16	0.931	
						68	(e) 2	358.963	2.03E-01	1.37E+08	-0.58	-0.60	0.950	
						2541	(e) 2	393.949	6.08E-06	4.11E+03	3.88E+03	-5.02	-5.04	0.001
						4803	(e) 2	432.500	2.19E-01	1.48E+08	1.40E+08	-0.38	-0.41	0.961
						10945	(e) 2	589.000	1.73E-04	1.17E+05	1.11E+05	-3.21	-3.24	0.214
						11736	(e) 0	617.822	4.66E-04	3.15E+05	2.98E+05	-2.74	-2.77	0.704
						12074	(e) 0	630.992	6.22E-03	4.20E+06	3.97E+06	-1.60	-1.63	0.611
						12102	(e) 1	632.085	4.22E-03	2.85E+06	2.69E+06	-1.77	-1.79	0.563
			12154	(e) 2	634.207	2.25E-04	1.52E+05	1.44E+05	-3.04	-3.06	0.323			
			25955	(e) 0	5093.945	6.48E-08	4.38E+01	4.14E+01	-4.72	-4.79	0.157			
			28021	(o) 2	4.7 <sup>d</sup>	0	(e) 1	356.770	1.39E-01	1.57E+08	-0.52	-0.55	0.950	

Table 6. Continued.

Upper level <sup>a</sup>	$\tau_u$ (ns)	Lower level <sup>a</sup>	$\lambda^b$ (nm)	<i>BF</i>	$gA$ (s <sup>-1</sup> )	$gA_{\text{resc}}$ (s <sup>-1</sup> )	$\log(gf)$	$\log(gf)_{\text{resc}}$	CF <sup>c</sup>
28161 (o) 3	4.7 <sup>d</sup>	68	357.634	5.02E-01	5.68E+08	5.34E+08	0.04	0.01	0.857
		178	359.047	1.27E-01	1.44E+08	1.35E+08	-0.55	-0.58	0.923
		2541	392.348	2.16E-03	2.44E+06	2.29E+06	-2.25	-2.28	0.741
		4803	430.571	2.13E-02	2.41E+07	2.26E+07	-1.17	-1.20	0.721
		4884	432.073	1.98E-01	2.24E+08	2.10E+08	-0.20	-0.23	0.963
		10945	585.430	8.92E-07	1.01E+03	9.49E+02	-5.28	-5.31	0.002
		12102	627.975	8.83E-03	1.00E+07	9.40E+06	-1.23	-1.25	0.651
		12154	630.070	2.24E-03	2.54E+06	2.39E+06	-1.82	-1.85	0.443
		68	355.853	1.18E-01	1.88E+08	1.76E+08	-0.45	-0.48	0.968
		178	357.253	6.52E-01	1.04E+09	9.72E+08	0.30	0.27	0.894
		2541	390.206	2.31E-05	3.69E+04	3.45E+04	-4.08	-4.10	0.023
		4803	427.993	3.06E-04	4.88E+05	4.56E+05	-2.87	-2.90	0.383
29736 (o) 0	7.7 <sup>d</sup>	4884	429.477	1.37E-02	2.18E+07	2.04E+07	-1.22	-1.25	0.601
		4988	431.408	2.04E-01	3.26E+08	3.05E+08	-0.04	-0.07	0.963
		10945	580.673	1.57E-04	2.50E+05	2.34E+05	-2.90	-2.93	0.555
		12154	624.564	1.10E-02	1.76E+07	1.64E+07	-1.02	-1.02	0.638
		14261	719.234	3.06E-05	4.88E+04	4.56E+04	-3.42	-3.45	0.419
		0	336.193	8.75E-01	1.38E+08	1.14E+08	-0.63	-0.72	0.519
		12102	566.904	1.25E-01	1.98E+07	1.63E+07	-1.02	-1.10	0.885
		0	336.127	2.43E-01	1.14E+08	9.57E+07	-0.72	-0.79	0.538
		68	336.894	6.21E-01	2.92E+08	2.45E+08	-0.30	-0.38	0.485
		2541	367.526	4.00E-03	1.88E+06	1.58E+06	-2.42	-2.49	0.070
		4803	400.860	2.21E-04	1.04E+05	8.73E+04	-3.60	-3.68	0.479
		10945	531.835	8.60E-03	4.04E+06	3.39E+06	-1.77	-1.84	0.723
29742 (o) 1	7.6 <sup>d</sup>	11736	555.222	5.30E-03	2.49E+06	2.09E+06	-1.94	-2.01	0.771
		12074	565.836	3.72E-02	1.75E+07	1.47E+07	-1.08	-1.15	0.736
		12102	566.715	3.19E-02	1.50E+07	1.26E+07	-1.15	-1.22	0.881
		12154	568.420	4.89E-02	2.30E+07	1.93E+07	-0.96	-1.03	0.813
		25955	639.920	7.02E-06	3.30E+03	2.77E+03	-3.46	-3.54	0.175
		0	335.205	1.05E-02	8.36E+06	7.12E+06	-1.85	-1.92	0.529
		68	335.968	1.47E-01	1.17E+08	9.96E+07	-0.71	-0.77	0.537
		178	337.215	7.13E-01	5.66E+08	4.82E+08	-0.02	-0.09	0.506
		2541	366.425	2.42E-03	1.92E+06	1.63E+06	-2.42	-2.48	0.731
		4803	399.550	3.24E-05	2.57E+04	2.19E+04	-4.21	-4.28	0.865
		4884	400.843	1.69E-04	1.34E+05	1.14E+05	-3.49	-3.56	0.912
		10945	529.531	4.02E-04	3.19E+05	2.72E+05	-2.88	-2.94	0.210
30816 (o) 1	8.8 <sup>d</sup>	12102	564.100	3.08E-02	2.44E+07	2.08E+07	-0.94	-1.00	0.825
		12154	565.790	9.49E-02	7.53E+07	6.41E+07	-0.45	-0.51	0.879
		0	324.416	7.98E-04	2.95E+05	2.72E+05	-3.33	-3.37	0.025
		68	325.131	2.31E-02	8.56E+06	7.89E+06	-1.87	-1.90	0.259
		2541	353.571	4.73E-01	1.75E+08	1.61E+08	-0.49	-0.52	0.193
		4803	384.317	2.68E-04	9.91E+04	9.14E+04	-3.66	-3.69	0.065
		10945	503.102	3.62E-01	1.34E+08	1.24E+08	-0.29	-0.33	0.723
		11736	523.981	1.24E-01	4.60E+07	4.24E+07	-0.72	-0.76	0.685

Table 6. Continued.

Upper level <sup>a</sup>	$\tau_u$ (ns)	Lower level <sup>a</sup>	$\lambda^b$ (nm)	$BF$	$gA$ (s <sup>-1</sup> )	$gA_{\text{resc}}$ (s <sup>-1</sup> )	$\log(gf)$	$\log(gf)_{\text{resc}}$	CF <sup>c</sup>	
12074		(e)	0	533.424	8.14E-03	3.01E+06	-1.89	-1.93	0.773	
12102		(e)	1	534.205	7.73E-04	2.86E+05	-2.91	-2.95	0.422	
12154		(e)	2	535.720	6.06E-03	2.24E+06	-2.01	-2.05	0.758	
25955		(e)	0	2056.840	8.71E-04	3.22E+05	-1.67	-1.73	0.214	
32350	(o)	3	5.1 <sup>d</sup>	68	309.678	5.40E-04	7.41E+05	-2.94	-2.97	0.182
		(e)	2	178	310.737	5.99E-04	8.22E+05	-2.89	-2.92	0.835
		(e)	2	2541	335.372	7.22E-01	1.08E+09	0.26	0.22	0.640
		(e)	2	4803	362.911	2.65E-04	3.96E+05	-3.11	-3.14	0.722
		(e)	3	4884	363.977	1.13E-05	1.69E+04	-4.47	-4.51	0.411
		(e)	4	4988	365.364	9.09E-05	1.36E+05	-3.57	-3.60	0.222
		(e)	2	10945	467.041	8.42E-02	1.26E+08	-0.39	-0.42	0.625
		(e)	2	12154	495.020	4.18E-04	6.25E+05	-2.64	-2.68	0.621
		(e)	4	14261	552.679	1.92E-01	2.88E+08	0.12	0.08	0.917
39002	(o)	0	3.7 <sup>d</sup>	0	256.319	9.94E-01	2.70E+08	-0.58	-0.58	0.958
		(e)	1	12102	371.632	5.85E-03	1.59E+06	-2.48	-2.48	0.139
39115	(o)	1	3.7 <sup>d</sup>	0	255.580	2.50E-01	2.04E+08	-0.70	-0.70	0.958
		(e)	1	68	256.023	7.41E-01	6.04E+08	-0.23	-0.23	0.955
		(e)	2	2541	273.337	4.16E-04	3.39E+05	-3.42	-3.42	0.244
		(e)	2	4803	291.357	4.23E-07	3.43E+02	-6.36	-6.36	0.362
		(e)	2	10945	354.880	2.80E-05	2.28E+04	-4.37	-4.37	0.095
		(e)	2	11736	365.144	5.13E-07	4.16E+02	-6.08	-6.08	0.001
		(e)	0	12074	369.704	1.94E-03	1.57E+06	-2.49	-2.49	0.137
		(e)	1	12102	370.079	1.44E-03	1.17E+06	-2.62	-2.62	0.137
		(e)	2	12154	370.806	2.36E-03	1.92E+06	-2.40	-2.40	0.136
39346	(o)	2	3.8 <sup>d</sup>	0	759.679	5.27E-07	4.27E+02	-5.43	-5.43	0.074
		(e)	1	68	254.082	1.02E-02	1.34E+07	-1.88	-1.89	0.957
		(e)	2	178	254.520	1.50E-01	1.98E+08	-0.70	-0.72	0.957
		(e)	3	2541	255.235	8.34E-01	1.10E+09	0.04	0.03	0.956
		(e)	2	4803	271.625	2.29E-04	3.01E+05	-3.47	-3.48	0.829
		(e)	2	4884	289.412	1.49E-07	2.02E+02	-6.60	-6.61	0.745
		(e)	3	10945	290.090	4.46E-07	6.05E+02	-6.12	-6.13	0.917
		(e)	2	12102	352.000	2.32E-05	3.14E+04	-4.23	-4.25	0.097
		(e)	1	12154	366.949	1.36E-03	1.80E+06	-2.43	-2.44	0.129
57744	(e)	3	3.20 <sup>e</sup>	0	367.663	4.12E-03	5.42E+06	-1.95	-1.96	0.132
		(o)	2	26081	315.739	5.95E-06	1.30E+04	-4.75	-4.71	0.004
		(o)	2	27444	329.936	1.75E-03	3.82E+06	-2.25	-2.21	0.660
		(o)	3	27602	331.673	4.87E-02	1.07E+08	-0.80	-0.75	0.694
		(o)	4	27841	334.323	3.77E-01	8.24E+08	0.10	0.14	0.668
		(o)	2	28021	336.347	5.55E-02	1.11E+08	-0.73	-0.69	0.851
		(o)	3	28161	337.938	3.93E-01	8.60E+08	0.13	0.17	0.834
		(o)	2	29824	358.064	1.24E-01	2.70E+08	-0.32	-0.28	0.458
		(o)	3	32350	393.683	8.95E-05	1.96E+05	-3.38	-3.34	0.357
		(o)	2	39346	543.375	5.65E-04	1.24E+06	-2.30	-2.26	0.027
58252	(e)	2	3.26 <sup>e</sup>	0	310.751	3.70E-01	4.99E+08	-0.14	-0.09	0.549

Upper level <sup>a</sup>	$\tau_u$ (ns)	Lower level <sup>a</sup>	$\lambda^b$ (nm)	<i>BF</i>	$gA$ (s <sup>-1</sup> )	$gA_{\text{resc}}$ (s <sup>-1</sup> )	$\log(gf)$	$\log(gf)_{\text{resc}}$	CF <sup>c</sup>
59528 (e)	2.32 <sup>e</sup>	27444 (o)	324.493	9.48E-03	1.28E+07	1.45E+07	-1.70	-1.64	0.583
		27602 (o)	326.174	7.63E-03	1.03E+07	1.17E+07	-1.79	-1.73	0.542
		27918 (o)	329.565	3.92E-04	5.29E+05	6.01E+05	-3.07	-3.01	0.062
		28021 (o)	330.693	1.11E-02	1.50E+07	1.70E+07	-1.61	-1.55	0.754
		28161 (o)	332.231	7.48E-04	1.01E+06	1.15E+06	-2.78	-2.72	0.136
		29742 (o)	350.655	4.07E-04	5.50E+05	6.25E+05	-2.99	-2.94	0.016
		29824 (o)	351.663	1.91E-03	2.58E+06	2.93E+06	-2.32	-2.26	0.439
		30816 (o)	364.376	1.56E-01	2.10E+08	2.39E+08	-0.38	-0.32	0.524
		32350 (o)	385.960	4.43E-01	5.98E+08	6.79E+08	0.13	0.18	0.811
		39115 (o)	522.401	6.04E-07	8.16E+02	9.27E+02	-5.48	-5.42	0.001
		39346 (o)	528.770	5.48E-06	7.40E+03	8.41E+03	-4.51	-4.45	0.032
		55715 (o)	3941.008	1.07E-04	1.45E+05	1.65E+05	-1.48	-1.42	0.272
		26081 (o)	298.893	7.30E-01	1.90E+09	2.20E+09	0.41	0.47	0.813
		27444 (o)	311.585	5.11E-04	1.33E+06	1.54E+06	-2.71	-2.65	0.017
		27602 (o)	313.134	1.28E-03	3.34E+06	3.87E+06	-2.31	-2.24	0.483
		27841 (o)	315.495	1.30E-03	3.38E+06	3.92E+06	-2.30	-2.23	0.444
		28021 (o)	317.297	8.37E-05	2.18E+05	2.53E+05	-3.48	-3.42	0.013
28161 (o)	318.712	7.76E-03	2.02E+07	2.34E+07	-1.51	-1.45	0.493		
29824 (o)	336.553	2.29E-03	5.97E+06	6.92E+06	-1.99	-1.93	0.229		
32350 (o)	367.834	2.57E-01	6.69E+08	7.75E+08	0.14	0.20	0.867		
39346 (o)	495.331	1.85E-04	4.81E+05	5.57E+05	-2.75	-2.69	0.621		
26081 (o)	295.826	1.55E-02	1.71E+07	2.09E+07	-1.64	-1.56	0.658		
27444 (o)	308.254	1.22E-01	1.34E+08	1.64E+08	-0.72	-0.63	0.631		
27918 (o)	312.827	3.93E-01	4.33E+08	5.29E+08	-0.20	-0.11	0.597		
28021 (o)	313.843	1.12E-01	1.23E+08	1.50E+08	-0.74	-0.65	0.481		
29736 (o)	331.703	1.92E-01	2.11E+08	2.58E+08	-0.46	-0.37	0.899		
29742 (o)	331.768	1.42E-01	1.57E+08	1.92E+08	-0.59	-0.50	0.750		
29824 (o)	332.670	7.03E-03	7.74E+06	9.45E+06	-1.89	-1.80	0.463		
30816 (o)	344.024	9.17E-04	1.01E+06	1.23E+06	-2.75	-2.66	0.021		
39002 (o)	478.957	9.08E-03	1.00E+07	1.22E+07	-1.46	-1.38	0.769		
39115 (o)	481.560	6.81E-03	7.50E+06	9.16E+06	-1.58	-1.50	0.766		
39346 (o)	486.967	3.60E-04	3.97E+05	4.85E+05	-2.85	-2.76	0.542		
55715 (o)	2403.352	2.00E-05	2.20E+04	2.69E+04	-2.72	-2.63	0.500		
26081 (o)	295.351	5.27E-05	9.68E+04	1.14E+05	-3.89	-3.83	0.011		
27444 (o)	307.738	9.53E-03	1.75E+07	2.05E+07	-1.61	-1.53	0.294		
27602 (o)	309.249	1.16E-01	2.13E+08	2.50E+08	-0.52	-0.45	0.667		
27918 (o)	312.296	7.46E-02	1.37E+08	1.61E+08	-0.70	-0.63	0.512		
28021 (o)	313.309	3.62E-01	6.64E+08	7.79E+08	-0.01	0.06	0.578		
28161 (o)	314.688	6.48E-02	1.19E+08	1.40E+08	-0.76	-0.68	0.420		
29742 (o)	331.170	2.71E-01	4.97E+08	5.83E+08	-0.09	-0.02	0.907		
29824 (o)	332.069	7.73E-02	1.42E+08	1.67E+08	-0.63	-0.56	0.690		
30816 (o)	343.382	3.84E-03	7.06E+06	8.29E+06	-1.91	-1.83	0.362		
32350 (o)	362.485	4.89E-06	8.98E+03	1.05E+04	-4.75	-4.68	0.022		
39115 (o)	480.302	1.24E-02	2.28E+07	2.68E+07	-1.10	-1.03	0.783		

Table 6. Continued.

Table 6. Continued.

Upper level <sup>a</sup>	$\tau_u$ (ns)	Lower level <sup>a</sup>	$\lambda^b$ (nm)	$BF$	$gA$ (s <sup>-1</sup> )	$gA_{\text{resc}}$ (s <sup>-1</sup> )	$\log(gf)$	$\log(gf)_{\text{resc}}$	CF <sup>c</sup>		
60002 (e) 3	2.41 <sup>e</sup>	39346 (o) 2	485.680	3.79E-03	6.96E+06	8.17E+06	-1.61	-1.54	0.716		
		55715 (o) 1	2372.344	1.32E-09	2.42E+00	2.84E+00	-6.69	-6.62	0.003		
		26081 (o) 2	294.720	5.91E-03	1.50E+07	1.72E+07	-1.71	-1.65	0.241		
		27444 (o) 2	307.053	9.57E-04	2.43E+06	2.78E+06	-2.47	-2.41	0.144		
		27602 (o) 3	308.558	3.10E-03	7.86E+06	9.00E+06	-1.95	-1.89	0.088		
		27841 (o) 4	310.850	1.09E-01	2.76E+08	3.16E+08	-0.40	-0.34	0.677		
		28021 (o) 2	312.599	5.52E-02	1.40E+08	1.60E+08	-0.69	-0.63	0.476		
		28161 (o) 3	313.972	4.41E-01	1.12E+09	1.28E+09	0.22	0.28	0.569		
		29824 (o) 2	331.272	3.63E-01	9.22E+08	1.06E+09	0.18	0.24	0.916		
		32350 (o) 3	361.535	5.75E-03	1.46E+07	1.67E+07	-1.54	-1.48	0.807		
60267 (e) 3	2.19 <sup>e</sup>	39346 (o) 2	483.977	1.58E-02	4.00E+07	4.58E+07	-0.85	-0.79	0.794		
		26081 (o) 2	292.433	2.06E-03	5.78E+06	6.59E+06	-2.13	-2.07	0.062		
		27444 (o) 2	304.572	9.17E-01	2.57E+09	2.93E+09	0.55	0.61	0.862		
		27602 (o) 3	306.052	7.60E-02	2.13E+08	2.43E+08	-0.52	-0.47	0.784		
		27841 (o) 4	308.307	7.21E-04	2.02E+06	2.30E+06	-2.54	-2.48	0.321		
		28021 (o) 2	310.027	1.66E-03	4.65E+06	5.30E+06	-2.17	-2.12	0.469		
		28161 (o) 3	311.378	9.67E-04	2.71E+06	3.09E+06	-2.40	-2.35	0.618		
		29824 (o) 2	328.386	2.14E-04	5.99E+05	6.83E+05	-3.01	-2.96	0.858		
		32350 (o) 3	358.100	1.44E-03	4.03E+06	4.60E+06	-2.11	-2.05	0.870		
		39346 (o) 2	477.840	6.67E-06	1.87E+04	2.13E+04	-4.19	-4.14	0.781		
60348 (e) 4	2.4 <sup>d</sup>	27602 (o) 3	305.292	9.37E-01	3.35E+09	3.52E+09	0.67	0.69	0.863		
		27841 (o) 4	307.536	5.82E-02	2.08E+08	2.18E+08	-0.53	-0.51	0.781		
		28161 (o) 3	310.592	4.25E-03	1.52E+07	1.60E+07	-1.66	-1.64	0.846		
		32350 (o) 3	357.060	7.98E-05	2.85E+05	2.99E+05	-3.26	-3.24	0.295		
		26081 (o) 2	291.298	2.97E-01	3.08E+08	3.65E+08	-0.41	-0.33	0.746		
		27444 (o) 2	303.340	1.18E-02	1.23E+07	1.46E+07	-1.77	-1.70	0.731		
		27918 (o) 1	307.767	2.40E-03	2.49E+06	2.95E+06	-2.45	-2.38	0.076		
		28021 (o) 2	308.751	4.66E-03	4.84E+06	5.73E+06	-2.16	-2.09	0.499		
		29736 (o) 0	326.020	1.01E-02	1.05E+07	1.24E+07	-1.78	-1.70	0.891		
		29742 (o) 1	326.082	1.70E-02	1.76E+07	2.08E+07	-1.55	-1.48	0.255		
60400 (e) 1	2.44 <sup>e</sup>	29824 (o) 2	326.955	3.85E-03	4.00E+06	4.74E+06	-2.19	-2.12	0.314		
		30816 (o) 1	337.915	6.51E-01	6.76E+08	8.01E+08	0.06	0.14	0.880		
		39002 (o) 0	467.198	5.28E-04	5.48E+05	6.49E+05	-2.75	-2.67	0.735		
		39115 (o) 1	469.675	1.63E-05	1.69E+04	2.00E+04	-4.26	-4.18	0.014		
		39346 (o) 2	474.816	3.58E-04	3.72E+05	4.41E+05	-2.90	-2.83	0.590		
		55715 (o) 1	2133.866	1.43E-03	1.48E+06	1.75E+06	-1.00	-0.92	0.554		
		27841 (o) 4	306.511	1.00E+00	4.33E+09	4.40E+09	0.79	0.79	0.865		
		26081 (o) 2	285.711	6.87E-04	7.30E+05	8.41E+05	-3.05	-2.99	0.084		
		27444 (o) 2	297.287	1.30E-05	1.38E+04	1.59E+04	-4.74	-4.68	0.061		
		27918 (o) 1	301.538	8.24E-05	8.76E+04	1.01E+05	-3.93	-3.86	0.091		
60457 (e) 5	2.5 <sup>d</sup>	28021 (o) 2	302.483	6.95E-05	7.39E+04	8.51E+04	-4.00	-3.93	0.056		
		29736 (o) 0	319.038	1.06E-01	1.13E+08	1.30E+08	-0.76	-0.70	0.841		
		29742 (o) 1	319.098	3.00E-01	3.19E+08	3.68E+08	-0.31	-0.25	0.802		
		29824 (o) 2	319.933	5.06E-01	5.38E+08	6.20E+08	-0.08	-0.02	0.837		
		61071 (e) 1	2.45 <sup>e</sup>	27841 (o) 4	306.511	1.00E+00	4.33E+09	4.40E+09	0.79	0.79	0.865
				26081 (o) 2	285.711	6.87E-04	7.30E+05	8.41E+05	-3.05	-2.99	0.084
				27444 (o) 2	297.287	1.30E-05	1.38E+04	1.59E+04	-4.74	-4.68	0.061
				27918 (o) 1	301.538	8.24E-05	8.76E+04	1.01E+05	-3.93	-3.86	0.091
				28021 (o) 2	302.483	6.95E-05	7.39E+04	8.51E+04	-4.00	-3.93	0.056
				29736 (o) 0	319.038	1.06E-01	1.13E+08	1.30E+08	-0.76	-0.70	0.841
29742 (o) 1	319.098			3.00E-01	3.19E+08	3.68E+08	-0.31	-0.25	0.802		
29824 (o) 2	319.933			5.06E-01	5.38E+08	6.20E+08	-0.08	-0.02	0.837		

Upper level <sup>a</sup>	$\tau_u$ (ns)	Lower level <sup>a</sup>	$\lambda^b$ (nm)	<i>BF</i>	$gA$ (s <sup>-1</sup> )	$gA_{\text{resc}}$ (s <sup>-1</sup> )	$\log(gf)$	$\log(gf)_{\text{resc}}$	CF <sup>c</sup>
63375 (e)	2.15 <sup>e</sup>	30816 (o)	330.421	2.64E-02	2.81E+07	3.24E+07	-1.34	-1.28	0.895
		39002 (o)	452.993	6.99E-03	7.43E+06	8.56E+06	-1.64	-1.58	0.718
		39115 (o)	455.321	2.08E-02	2.21E+07	2.55E+07	-1.17	-1.10	0.750
		39346 (o)	460.151	3.23E-02	3.43E+07	3.95E+07	-0.96	-0.90	0.742
		55715 (o)	1866.531	1.98E-05	2.10E+04	2.42E+04	-2.96	-2.90	0.528
		26081 (o)	268.065	1.38E-02	2.88E+07	3.21E+07	-1.51	-1.46	0.561
		27444 (o)	278.230	3.17E-01	6.61E+08	7.37E+08	-0.12	-0.07	0.673
		27602 (o)	279.464	4.12E-02	8.59E+07	9.58E+07	-1.00	-0.95	0.701
		27918 (o)	281.950	5.37E-01	1.12E+09	1.25E+09	0.12	0.17	0.685
		28021 (o)	282.776	8.92E-02	1.86E+08	2.07E+08	-0.65	-0.60	0.516
		28161 (o)	283.899	1.87E-03	3.91E+06	4.36E+06	-2.33	-2.28	0.263
		29742 (o)	297.245	3.20E-05	6.68E+04	7.45E+04	-4.05	-4.01	0.023
		29824 (o)	297.969	2.25E-05	4.70E+04	5.24E+04	-4.20	-4.16	0.075
		30816 (o)	307.046	2.30E-06	4.79E+03	5.34E+03	-5.17	-5.12	0.000
		32350 (o)	322.231	1.81E-04	3.77E+05	4.20E+05	-3.23	-3.18	0.221
39115 (o)	412.092	1.83E-06	3.81E+03	4.25E+03	-5.01	-4.97	0.218		
39346 (o)	416.045	3.25E-07	6.78E+02	7.56E+02	-5.76	-5.71	0.068		
55715 (o)	1305.250	5.75E-06	1.20E+04	1.34E+04	-3.51	-3.47	0.207		
63529 (e)	2.19 <sup>e</sup>	27602 (o)	278.267	7.54E-03	2.79E+07	3.10E+07	-1.49	-1.44	0.119
		27841 (o)	280.130	3.33E-01	1.23E+09	1.37E+09	0.16	0.21	0.704
		28161 (o)	282.663	6.60E-01	2.44E+09	2.71E+09	0.47	0.51	0.697
		32350 (o)	320.641	3.38E-05	1.25E+05	1.39E+05	-3.71	-3.67	0.014
		26081 (o)	261.119	5.63E-01	1.03E+09	1.25E+09	0.03	0.11	0.410
		27444 (o)	270.754	1.32E-02	2.41E+07	2.93E+07	-1.58	-1.49	0.444
		27602 (o)	271.923	5.47E-04	1.00E+06	1.21E+06	-2.96	-2.87	0.510
		27918 (o)	274.276	3.89E-04	7.11E+05	8.64E+05	-3.10	-3.01	0.023
		28021 (o)	275.057	4.30E-04	7.87E+05	9.56E+05	-3.05	-2.96	0.021
		28161 (o)	276.120	8.53E-03	1.56E+07	1.90E+07	-1.75	-1.66	0.258
		29742 (o)	288.728	3.03E-02	5.55E+07	6.74E+07	-1.16	-1.07	0.503
		29824 (o)	289.412	1.85E-02	3.38E+07	4.11E+07	-1.37	-1.29	0.305
		30816 (o)	297.967	3.20E-01	5.85E+08	7.11E+08	-0.11	-0.02	0.567
		32350 (o)	312.247	4.32E-02	7.90E+07	9.60E+07	-0.94	-0.85	0.207
		39115 (o)	395.902	3.40E-05	6.22E+04	7.56E+04	-3.84	-3.75	0.017
64706 (e)	2.51 <sup>e</sup>	39346 (o)	399.549	9.57E-05	1.75E+05	2.13E+05	-3.38	-3.29	0.021
		55715 (o)	1155.577	1.90E-03	3.48E+06	4.23E+06	-1.16	-1.07	0.207
		26081 (o)	258.825	2.19E-02	3.43E+07	4.36E+07	-1.46	-1.36	0.199
		27444 (o)	268.289	8.23E-04	1.29E+06	1.64E+06	-2.86	-2.75	0.238
		27602 (o)	269.437	6.38E-04	9.99E+05	1.27E+06	-2.97	-2.86	0.208
		27918 (o)	271.746	8.55E-04	1.34E+06	1.70E+06	-2.83	-2.72	0.055
		28021 (o)	272.513	2.21E-02	3.46E+07	4.40E+07	-1.42	-1.31	0.154
		28161 (o)	273.556	1.56E-01	2.44E+08	3.10E+08	-0.56	-0.46	0.252
		29742 (o)	285.927	1.63E-01	2.56E+08	3.26E+08	-0.50	-0.40	0.424
		29824 (o)	286.597	5.87E-01	9.20E+08	1.17E+09	0.06	0.16	0.545
		30816 (o)	294.984	4.05E-02	6.35E+07	8.07E+07	-1.08	-0.98	0.562

Table 6. Continued.

Table 6. Continued.

Upper level <sup>a</sup>	$\tau_u$ (ns)	Lower level <sup>a</sup>	$\lambda^b$ (nm)	$BF$	$gA$ (s <sup>-1</sup> )	$gA_{\text{resc}}$ (s <sup>-1</sup> )	$\log(gf)$	$\log(gf)_{\text{resc}}$	CF <sup>c</sup>		
74433 (e)	3.80 <sup>e</sup>	32350 (o)	308.973	3.45E-03	5.40E+06	6.87E+06	-2.11	-2.01	0.222		
		39115 (o)	390.654	7.53E-04	1.18E+06	1.50E+06	1.50E+06	-2.57	-2.46	0.021	
		39346 (o)	2	394.204	2.45E-03	3.84E+06	4.88E+06	4.88E+06	-2.05	-1.94	0.024
		55715 (o)	1	1111.977	1.19E-04	1.87E+05	2.38E+05	2.38E+05	-2.46	-2.36	0.198
		26081 (o)	2	206.751	7.13E-02	5.98E+07	9.38E+07	9.38E+07	-1.42	-1.22	0.047
		27444 (o)	2	212.746	1.00E-03	8.40E+05	1.32E+06	1.32E+06	-3.25	-3.05	0.054
		27602 (o)	3	213.467	5.58E-05	4.68E+04	7.34E+04	7.34E+04	-4.51	-4.30	0.083
		27918 (o)	1	214.914	8.51E-07	7.14E+02	1.12E+03	1.12E+03	-6.32	-6.11	0.000
		28021 (o)	2	215.394	2.11E-04	1.77E+05	2.78E+05	2.78E+05	-3.92	-3.71	0.024
		28161 (o)	3	216.045	1.07E-02	8.94E+06	1.40E+07	1.40E+07	-2.21	-2.01	0.455
		29742 (o)	1	223.689	5.46E-04	4.58E+05	7.19E+05	7.19E+05	-3.47	-3.27	0.005
		29824 (o)	2	224.099	2.39E-05	2.00E+04	3.14E+04	3.14E+04	-4.83	-4.63	0.001
		30816 (o)	1	229.195	4.05E-03	3.40E+06	5.34E+06	5.34E+06	-2.58	-2.38	0.002
		32350 (o)	3	237.551	8.23E-01	6.90E+08	1.08E+09	1.08E+09	-0.24	-0.04	0.251
		39115 (o)	1	283.056	2.83E-03	2.37E+06	3.72E+06	3.72E+06	-2.56	-2.35	0.244
		39346 (o)	2	284.916	1.05E-02	8.83E+06	1.39E+07	1.39E+07	-1.98	-1.77	0.660
		55715 (o)	1	534.098	4.13E-04	3.46E+05	5.43E+05	5.43E+05	-2.85	-2.63	0.000
		66048 (o)	2	1192.292	3.94E-02	3.30E+07	5.18E+07	5.18E+07	-0.20	0.04	0.693
		66390 (o)	1	1242.891	4.01E-05	3.36E+04	5.27E+04	5.27E+04	-3.17	-2.91	0.227
		66493 (o)	2	1259.000	6.15E-05	5.16E+04	8.10E+04	8.10E+04	-2.97	-2.72	0.112
66460 (o)	2	1253.786	1.25E-03	1.05E+06	1.65E+06	1.65E+06	-1.66	-1.41	0.403		
66564 (o)	3	1270.370	2.48E-04	2.08E+05	3.26E+05	3.26E+05	-2.36	-2.10	0.374		
66584 (o)	3	1273.628	8.54E-05	7.16E+04	1.12E+05	1.12E+05	-2.82	-2.56	0.390		
67298 (o)	1	1401.037	5.56E-05	4.66E+04	7.31E+04	7.31E+04	-2.93	-2.67	0.085		
67396 (o)	2	1420.650	7.89E-07	6.62E+02	1.04E+03	1.04E+03	-4.76	-4.50	0.003		
67744 (o)	3	1494.454	2.93E-02	2.46E+07	3.86E+07	3.86E+07	-0.15	0.11	0.695		
68498 (o)	1	1684.392	5.06E-03	4.24E+06	6.65E+06	6.65E+06	-0.82	-0.55	0.165		
26081 (o)	2	198.888	2.24E-04	5.75E+05	5.91E+05	5.91E+05	-3.47	-3.46	0.126		
27444 (o)	2	204.362	3.68E-04	9.44E+05	9.70E+05	9.70E+05	-3.23	-3.22	0.387		
27918 (o)	1	206.362	7.57E-02	1.94E+08	1.99E+08	1.99E+08	-0.91	-0.90	0.507		
28021 (o)	2	206.804	2.30E-01	5.88E+08	6.04E+08	6.04E+08	-0.42	-0.41	0.527		
29736 (o)	0	214.412	9.25E-05	2.37E+05	2.43E+05	2.43E+05	-3.79	-3.77	0.000		
29742 (o)	1	214.439	2.71E-04	6.93E+05	7.12E+05	7.12E+05	-3.32	-3.31	0.002		
29824 (o)	2	214.816	5.31E-05	1.36E+05	1.40E+05	1.40E+05	-4.03	-4.01	0.000		
30816 (o)	1	219.494	9.17E-05	2.35E+05	2.41E+05	2.41E+05	-3.77	-3.76	0.015		
39002 (o)	0	267.597	2.33E-01	5.96E+08	6.12E+08	6.12E+08	-0.19	-0.18	0.708		
39115 (o)	1	268.407	1.73E-01	4.44E+08	4.56E+08	4.56E+08	-0.32	-0.31	0.705		
39346 (o)	2	270.079	2.84E-01	7.28E+08	7.48E+08	7.48E+08	-0.10	-0.09	0.709		
55715 (o)	1	484.233	1.12E-06	2.88E+03	2.96E+03	2.96E+03	-5.00	-4.98	0.080		
66048 (o)	2	969.440	1.10E-05	2.83E+04	2.91E+04	2.91E+04	-3.40	-3.39	0.091		
66390 (o)	1	1002.628	2.87E-04	7.35E+05	7.55E+05	7.55E+05	-1.96	-1.94	0.402		
66493 (o)	2	1013.085	4.41E-04	1.13E+06	1.16E+06	1.16E+06	-1.76	-1.75	0.319		
66460 (o)	2	1009.706	1.72E-04	4.40E+05	4.52E+05	4.52E+05	-2.17	-2.16	0.307		
67237 (o)	0	1095.698	9.72E-04	2.49E+06	2.56E+06	2.56E+06	-1.35	-1.34	0.575		

**Table 6.** Continued.

Upper level <sup>a</sup>	$\tau_u$ (ns)	Lower level <sup>a</sup>	$\lambda^b$ (nm)	<i>BF</i>	$g_A$ (s <sup>-1</sup> )	$g_{A_{\text{resc}}}$ (s <sup>-1</sup> )	$\log(gf)$	$\log(gf)_{\text{resc}}$	CF <sup>c</sup>
67298		(o) 1	1103.071	6.87E-04	1.76E+06	1.81E+06	-1.49	-1.48	0.528
67396		(o) 2	1115.192	9.76E-04	2.50E+06	2.57E+06	-1.33	-1.32	0.472
68498		(o) 1	1271.473	3.72E-07	9.52E+02	9.78E+02	-4.64	-4.63	0.029
75308		(o) 2	9497.064	1.05E-07	2.69E+02	2.76E+02	-3.44	-3.43	0.567
75591		(o) 2	12984.147	3.27E-07	8.37E+02	8.60E+02	-2.68	-2.66	0.581
75651		(o) 1	14082.652	2.29E-07	5.87E+02	6.03E+02	-2.76	-2.75	0.295
75681		(o) 2	14699.495	9.76E-07	2.50E+03	2.57E+03	-2.10	-2.08	0.578
75913		(o) 2	22304.392	1.26E-08	3.22E+01	3.31E+01	-3.64	-3.61	0.035
75952		(o) 1	24447.995	4.84E-08	1.24E+02	1.27E+02	-2.97	-2.94	0.375
75994		(o) 0	27287.372	2.90E-08	7.44E+01	7.64E+01	-3.11	-3.07	0.363
76073		(o) 1	34770.709	1.85E-10	4.75E-01	4.88E-01	-5.04	-5.05	0.031
76589	(e) 2	1.09 <sup>e</sup>							
26081		(o) 2	197.989	1.79E-04	7.57E+05	8.23E+05	-3.35	-3.32	0.040
27444		(o) 2	203.412	7.58E-05	3.20E+05	3.48E+05	-3.70	-3.67	0.170
27602		(o) 3	204.071	1.10E-03	4.64E+06	5.04E+06	-2.54	-2.50	0.490
27918		(o) 1	205.393	3.08E-03	1.30E+07	1.41E+07	-2.08	-2.05	0.390
28021		(o) 2	205.831	4.50E-02	1.90E+08	2.07E+08	-0.92	-0.88	0.454
28161		(o) 3	206.426	2.51E-01	1.06E+09	1.15E+09	-0.17	-0.13	0.529
29742		(o) 1	213.393	1.33E-05	5.60E+04	6.09E+04	-4.42	-4.38	0.000
29824		(o) 2	213.766	4.74E-04	2.00E+06	2.17E+06	-2.86	-2.83	0.001
30816		(o) 1	218.398	1.25E-04	5.27E+05	5.73E+05	-3.42	-3.39	0.012
32350		(o) 3	225.973	1.25E-03	5.26E+06	5.72E+06	-2.39	-2.36	0.328
39115		(o) 1	266.771	1.77E-01	7.46E+08	8.11E+08	-0.10	-0.06	0.705
39346		(o) 2	268.422	5.17E-01	2.18E+09	2.37E+09	0.37	0.41	0.709
55715		(o) 1	478.932	2.35E-05	9.91E+04	1.08E+05	-3.47	-3.43	0.019
66048		(o) 2	948.425	2.61E-05	1.10E+05	1.20E+05	-2.82	-2.79	0.065
66390		(o) 1	980.166	1.23E-05	5.20E+04	5.65E+04	-3.13	-3.09	0.219
66493		(o) 2	990.157	1.52E-04	6.43E+05	6.99E+05	-2.03	-1.99	0.337
66460		(o) 2	986.929	6.09E-05	2.57E+05	2.79E+05	-2.42	-2.39	0.243
66564		(o) 3	997.176	6.97E-04	2.94E+06	3.20E+06	-1.36	-1.32	0.372
66584		(o) 3	999.182	1.61E-04	6.78E+05	7.37E+05	-1.99	-1.96	0.215
67298		(o) 1	1075.944	8.96E-04	3.78E+06	4.11E+06	-1.18	-1.15	0.593
67396		(o) 2	1087.473	2.06E-03	8.71E+06	9.47E+06	-0.81	-0.77	0.517
67744		(o) 3	1130.199	9.83E-05	4.15E+05	4.51E+05	-2.10	-2.06	0.549
68498		(o) 1	1235.566	1.70E-05	7.17E+04	7.79E+04	-2.78	-2.75	0.138
75308		(o) 2	7803.238	4.76E-08	2.01E+02	2.18E+02	-3.74	-3.70	0.536
75309		(o) 3	7806.711	2.44E-07	1.03E+03	1.12E+03	-3.03	-2.99	0.670
75373		(o) 3	8220.091	2.89E-07	1.22E+03	1.33E+03	-2.91	-2.87	0.502
75552		(o) 3	9642.061	1.18E-07	5.00E+02	5.43E+02	-3.16	-3.12	0.304
75591		(o) 2	10012.694	8.81E-09	3.72E+01	4.04E+01	-4.26	-4.22	0.012
75651		(o) 1	10653.532	2.30E-09	9.70E+00	1.05E+01	-4.79	-4.75	0.011
75681		(o) 2	11002.823	1.28E-07	5.40E+02	5.87E+02	-3.02	-2.97	0.092
75716		(o) 3	11444.422	2.21E-06	9.33E+03	1.01E+04	-1.75	-1.70	0.611
75913		(o) 2	14773.133	5.78E-07	2.44E+03	2.65E+03	-2.11	-2.06	0.445
75952		(o) 1	15683.966	1.11E-07	4.69E+02	5.10E+02	-2.78	-2.73	0.354



Table 6. Continued.

Upper level <sup>a</sup>	$\tau_u$ (ns)	Lower level <sup>a</sup>	$\lambda^b$ (nm)	$BF$	$gA$ (s <sup>-1</sup> )	$gA_{\text{resc}}$ (s <sup>-1</sup> )	$\log(gf)$	$\log(gf)_{\text{resc}}$	CF <sup>c</sup>
77387 (e) 3	3.73 <sup>e</sup>	76073 (o) 1	19373.811	7.70E-09	3.25E+01	3.53E+01	-3.73	-3.70	0.278
		26081 (o) 2	194.910	2.66E-05	3.37E+04	5.00E+04	-4.71	-4.55	0.015
		27444 (o) 2	200.162	8.78E-04	1.11E+06	1.65E+06	-3.17	-3.00	0.300
		27602 (o) 3	200.800	2.37E-02	3.00E+07	4.45E+07	-1.74	-1.57	0.312
		27841 (o) 4	201.768	2.02E-01	2.56E+08	3.80E+08	-0.80	-0.63	0.327
		28021 (o) 2	202.504	1.99E-02	2.52E+07	3.74E+07	-1.81	-1.64	0.293
		28161 (o) 3	203.079	1.29E-01	1.63E+08	2.42E+08	-0.99	-0.82	0.269
		29824 (o) 2	210.180	1.76E-01	2.23E+08	3.31E+08	-0.83	-0.66	0.374
		32350 (o) 3	221.970	4.87E-05	6.16E+04	9.14E+04	-4.34	-4.17	0.126
		39346 (o) 2	262.791	1.16E-01	1.47E+08	2.18E+08	-0.81	-0.65	0.249
		66048 (o) 2	881.687	2.62E-04	3.32E+05	4.93E+05	-2.39	-2.24	0.123
		66493 (o) 2	917.642	8.86E-03	1.12E+07	1.66E+07	-0.83	-0.68	0.509
		66460 (o) 2	914.869	6.78E-03	8.58E+06	1.27E+07	-0.95	-0.80	0.781
		66564 (o) 3	923.667	6.02E-02	7.62E+07	1.13E+08	0.01	0.16	0.379
		66584 (o) 3	925.388	7.61E-02	9.63E+07	1.43E+08	0.11	0.26	0.792
		66719 (o) 4	937.110	1.33E-01	1.68E+08	2.49E+08	0.36	0.52	0.748
		67396 (o) 2	1000.629	4.64E-02	5.87E+07	8.71E+07	-0.04	0.12	0.575
		67744 (o) 3	1036.689	4.70E-05	5.94E+04	8.81E+04	-3.00	-2.85	0.115
		75221 (o) 4	4616.186	1.04E-06	1.31E+03	1.94E+03	-3.28	-3.21	0.152
75308 (o) 2	4808.601	2.30E-08	2.91E+01	4.32E+01	-4.90	-4.82	0.068		
75309 (o) 3	4809.920	4.80E-08	6.07E+01	9.01E+01	-4.58	-4.50	0.011		
75373 (o) 3	4963.717	4.93E-07	6.24E+02	9.26E+02	-3.54	-3.47	0.150		
75390 (o) 4	5006.948	1.42E-06	1.80E+03	2.67E+03	-3.07	-3.00	0.104		
75470 (o) 4	5215.252	1.24E-06	1.57E+03	2.33E+03	-3.09	-3.02	0.112		
75552 (o) 3	5448.967	1.03E-06	1.30E+03	1.93E+03	-3.13	-3.07	0.538		
75561 (o) 4	5474.449	1.18E-08	1.49E+01	2.21E+01	-5.05	-5.00	0.107		
75591 (o) 2	5565.388	5.53E-07	7.00E+02	1.04E+03	-3.37	-3.32	0.306		
75681 (o) 2	5858.418	1.88E-06	2.38E+03	3.53E+03	-2.79	-2.74	0.571		
75716 (o) 3	5981.306	1.01E-05	1.28E+04	1.90E+04	-2.04	-1.99	0.848		
75913 (o) 2	6779.698	4.40E-07	5.56E+02	8.25E+02	-3.28	-3.24	0.072		

<sup>a</sup> Each level is designated by its value in cm<sup>-1</sup>, its parity ((e) and (o) stand for even and odd respectively) and its total quantum number,  $J$ .

<sup>b</sup> Calculated from the energy levels compiled by NIST (Kramida et al. 2015).  $\lambda > 200$  nm are given in air.

<sup>c</sup> Cancellation factor as defined by Cowan (1981). A value less than 5% indicates a strong cancellation effect on the line strength and the transition probability could be underestimated.

<sup>d</sup> TR-LIF measurements by Marsden et al. (1988).

<sup>e</sup> TR-LIF measurements. This work.

**Table 7.** Sc II lines used in the determination of the solar abundance ( $\log \epsilon$ ) of scandium.

Transition	$\lambda^a$ (nm)	$\log(gf)_{L\&D}^b$	$\log(gf)_{\text{resc}}^c$	$\Delta \log(gf)^d$	$\log \epsilon^e$	$\log \epsilon_{\text{cor}}^e$	Weight <sup>e</sup>
$3d^2 \ ^3F_4 - 3d4p \ ^3F_3^o$	442.067	-2.273	-1.950	0.323	3.099	2.776	2
$3d^2 \ ^3F_3 - 3d4p \ ^3F_2^o$	443.135	-1.969	-1.780	0.189	3.155	2.966	1
$3d^2 \ ^3P_2 - 3d4p \ ^1P_1^o$	535.720	-2.111	-2.050	0.061	3.131	3.070	2
$3d^2 \ ^3P_1 - 3d4p \ ^3P_2^o$	564.100	-1.131	-1.000	0.131	3.226	3.095	1
$3d^2 \ ^3P_0 - 3d4p \ ^3P_1^o$	565.836	-1.208	-1.150	0.058	3.211	3.153	1
$3d^2 \ ^3P_1 - 3d4p \ ^3P_0^o$	566.715	-1.309	-1.220	0.089	3.235	3.146	1
$3d^2 \ ^3P_1 - 3d4p \ ^3P_0^o$	566.904	-1.200	-1.100	0.100	3.246	3.146	1
$3d^2 \ ^3P_2 - 3d4p \ ^3P_1^o$	568.420	-1.074	-1.030	0.044	3.154	3.110	2
$3d^2 \ ^1D_2 - 3d4p \ ^1D_2^o$	660.460	-1.309	-1.570 <sup>g</sup>	-0.261	3.204	3.465	1

<sup>a</sup> Calculated from the energy levels compiled by NIST (Kramida et al. 2015).<sup>b</sup> Scott et al. (2015), deduced from the  $A$ -values of Lawler and Dakin (1989).<sup>c</sup> This work. Rescaled value.<sup>d</sup>  $\Delta \log(gf) = \log(gf)_{L\&D} - \log(gf)_{\text{resc}}$ .<sup>e</sup> Scott et al. (2015).<sup>f</sup> This work. Corrected abundance,  $\log \epsilon_{\text{cor}} = \log \epsilon - \Delta \log(gf)$ .<sup>g</sup> Affected by strong cancellation effects ( $CF < 0.05$ ).

This paper has been typeset from a  $\text{T}_{\text{E}}\text{X}/\text{L}^{\text{A}}\text{T}_{\text{E}}\text{X}$  file prepared by the author.